Off-shell 4ℓ Higgs boson measurements @ CMS and ATLAS

Ulascan Sarica
UC SANTA BARBARA

U.S. DEPARTMENT OF ENERGY
Office of Science

SM@LHC ‘23
Jul. 10, 2023

Why measure the Higgs boson width?

Are there subdominant contributions to our current production and decay calculations we have not yet included?

Does the Higgs boson interact with particles we cannot detect (e.g. neutrinos)?

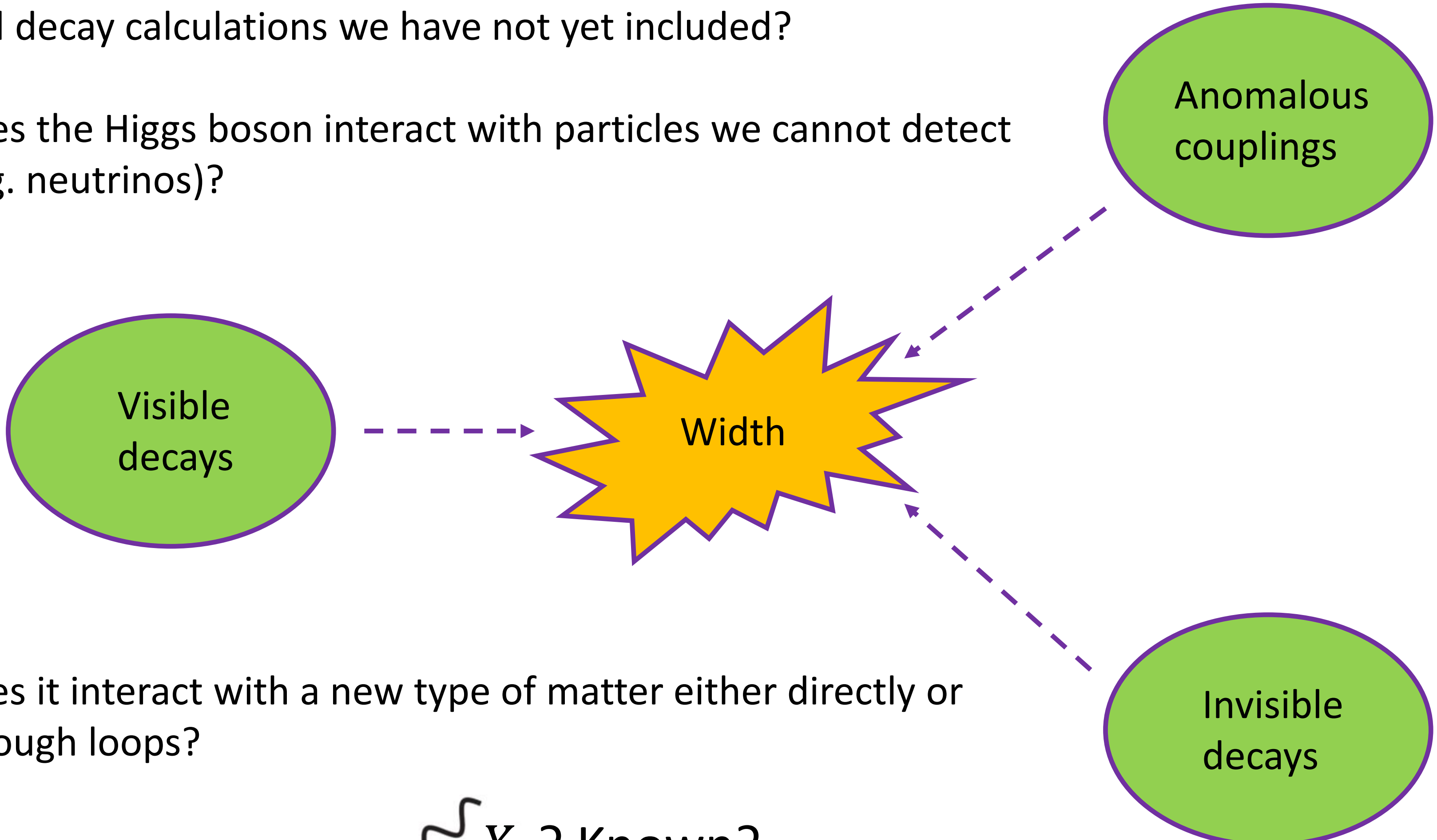

Does it interact with a new type of matter either directly or through loops?

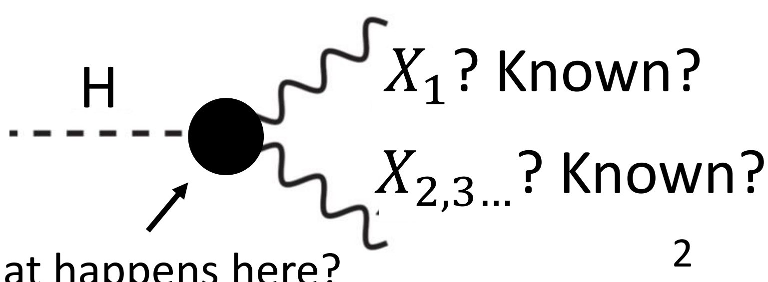

What can we measure?

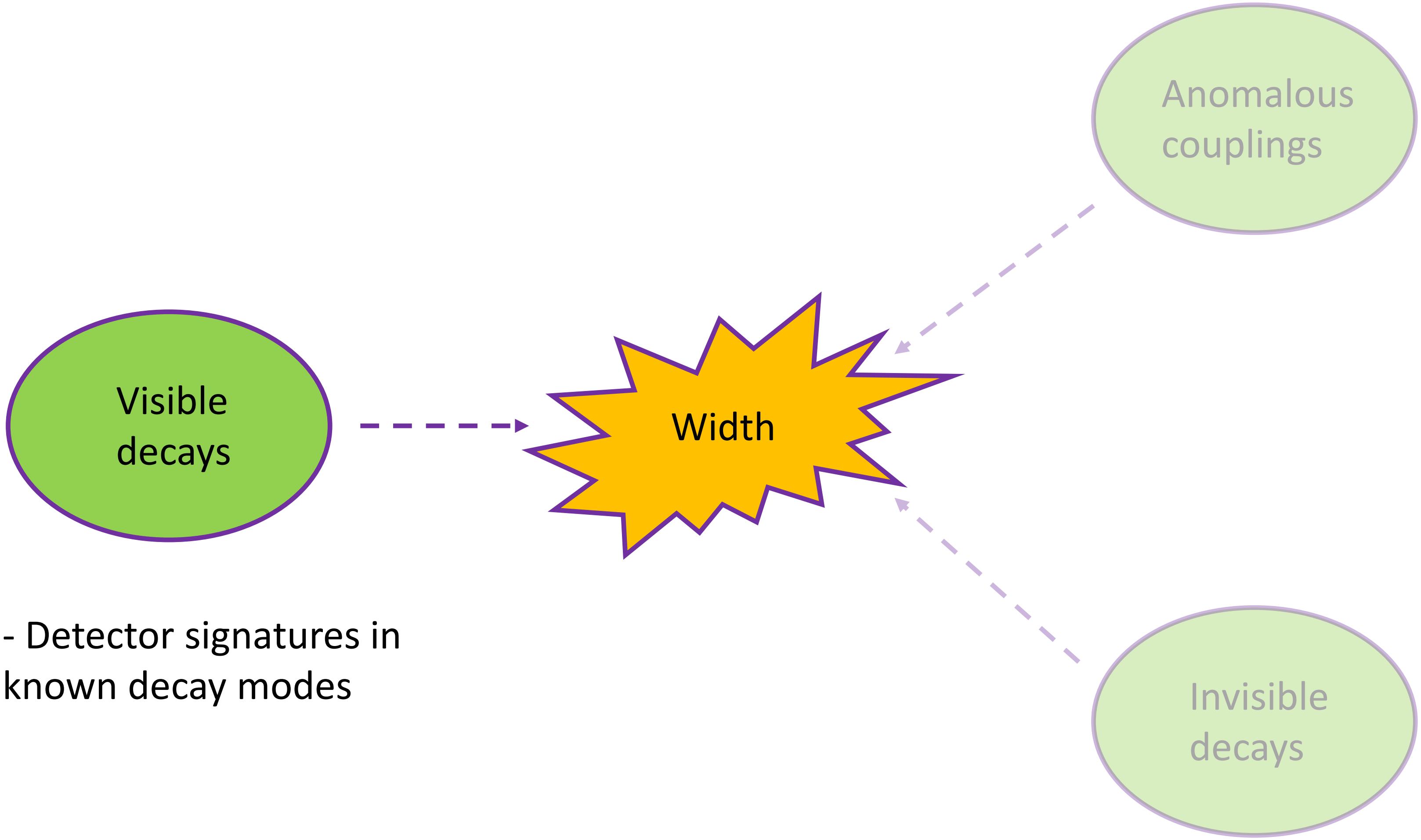

- Detector signatures in known decay modes

What can we measure?

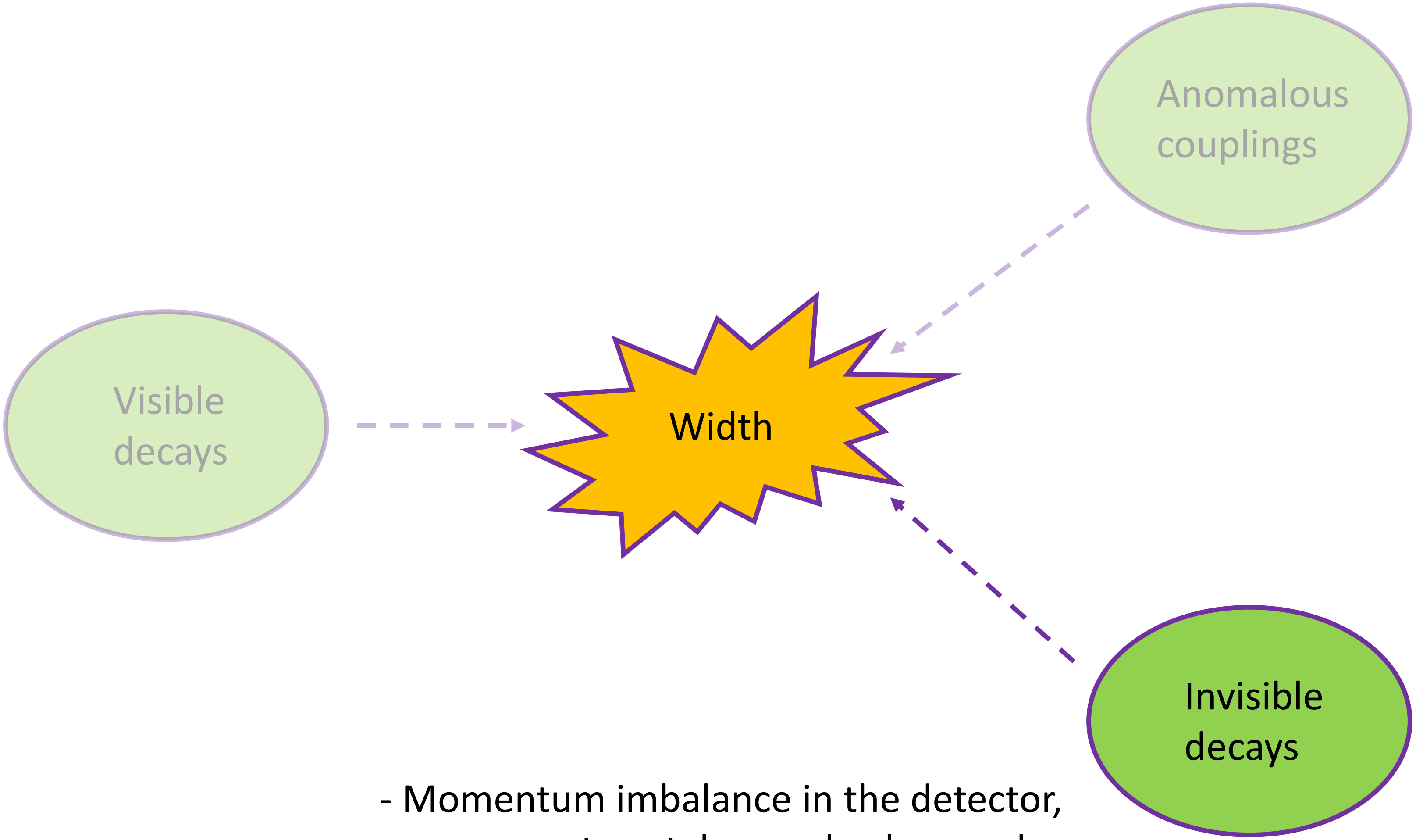

- Momentum imbalance in the detector, excess events wrt. known backgrounds

What can we measure?

- Angular and mass observables
- Production and decay correlations

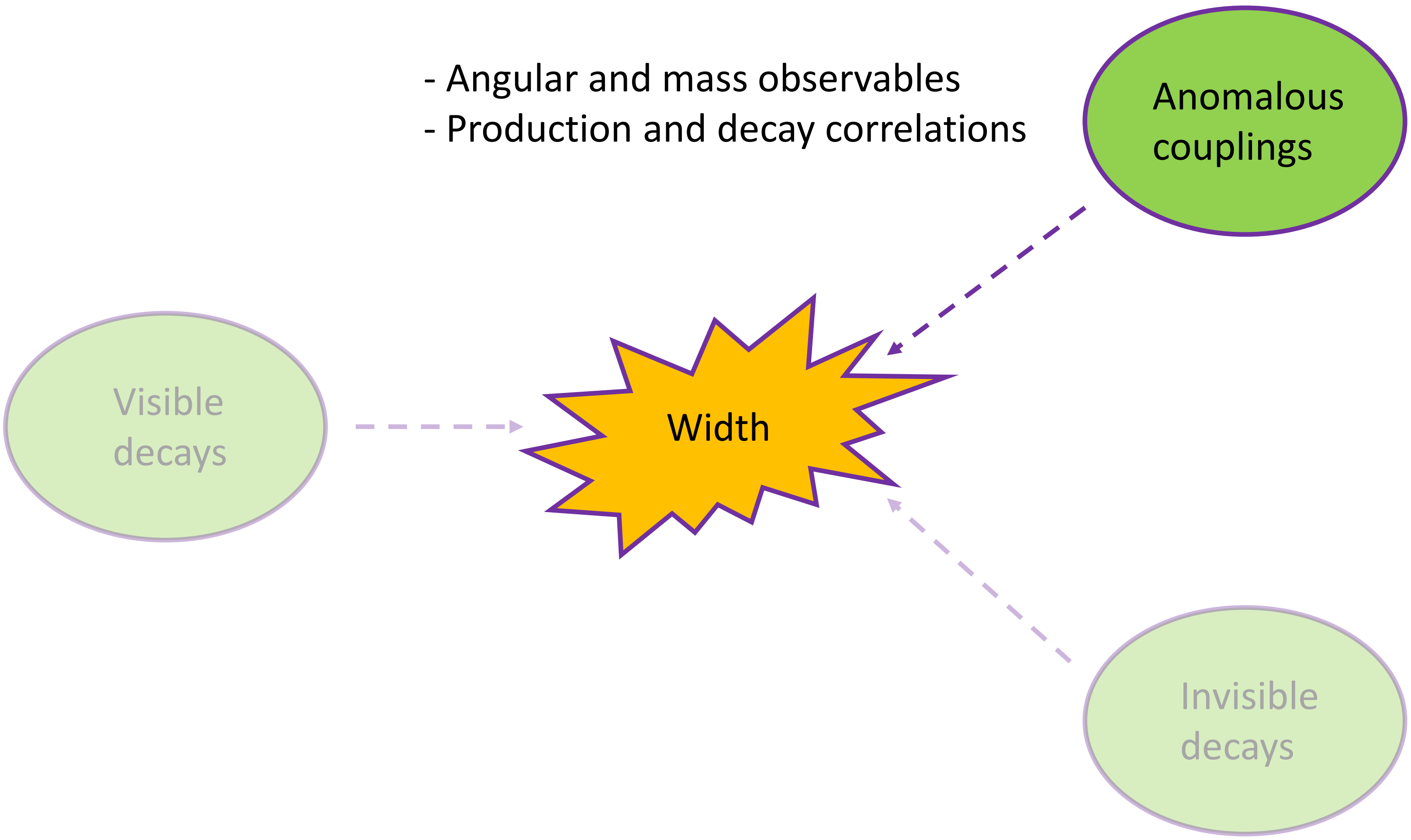

What can we measure?

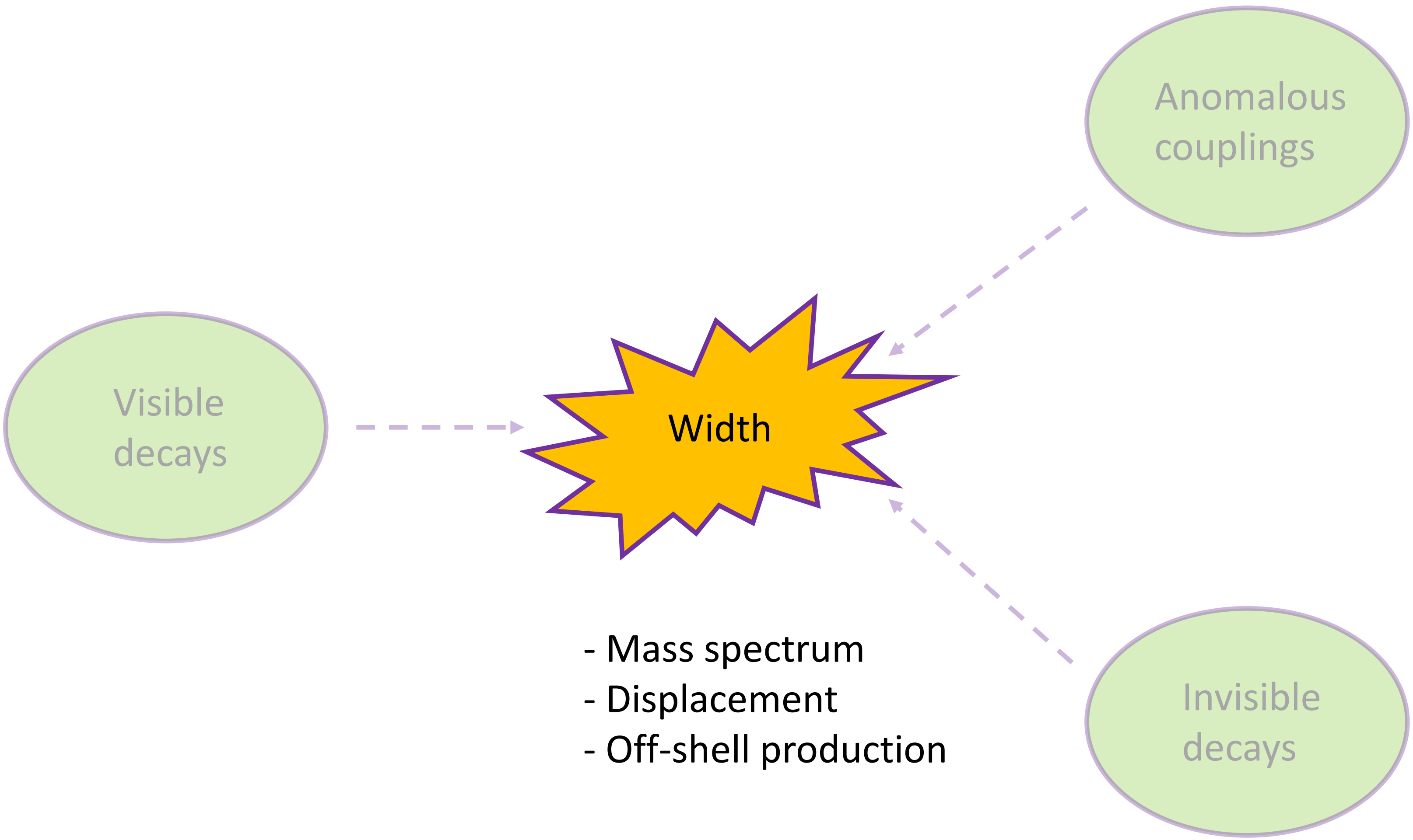

- Mass spectrum
- Displacement
- Off-shell production

What can we measure?

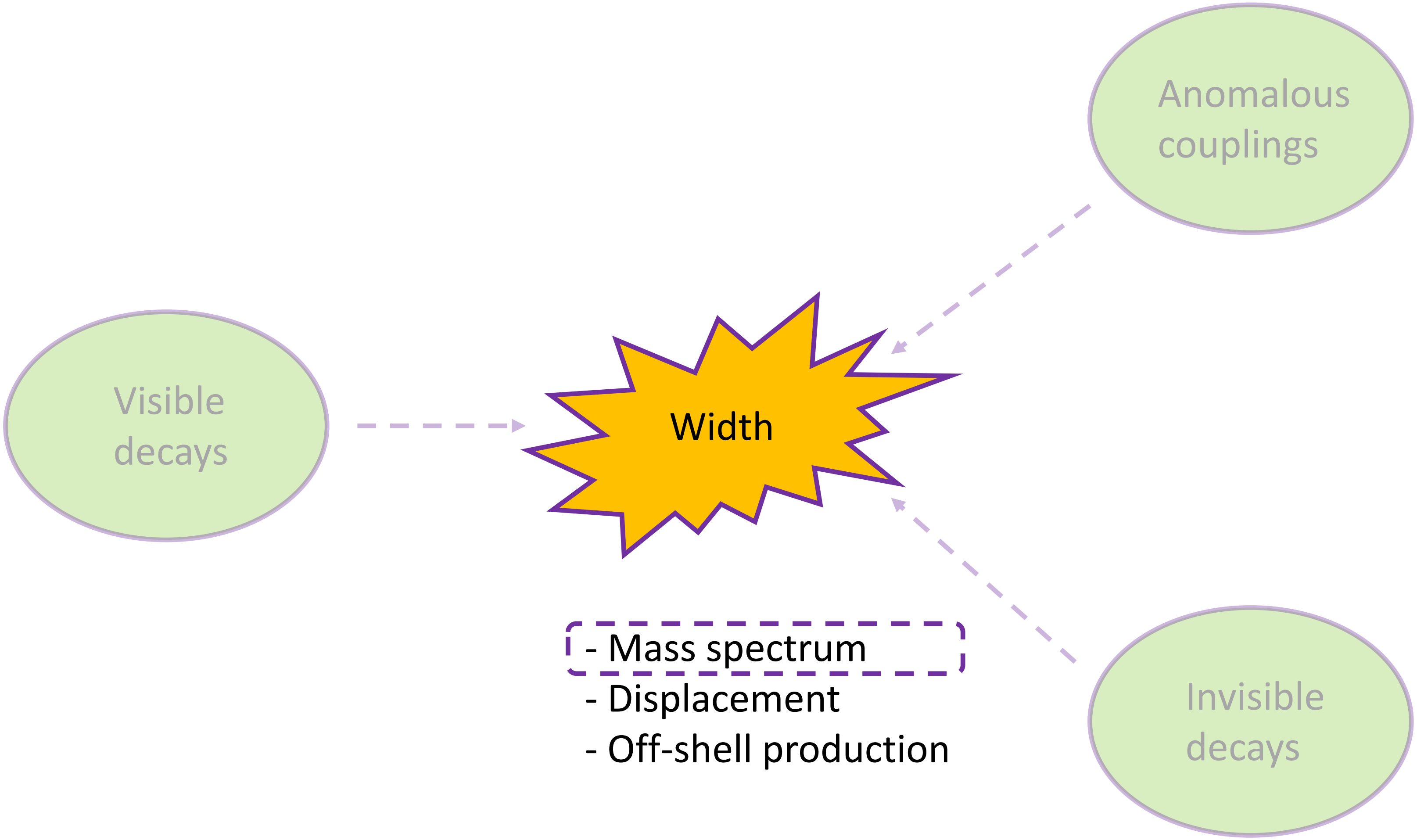

- Mass spectrum
- Displacement
- Off-shell production

SM: 4.1 MeV
Detector resolution: ~1 GeV

What can we measure?

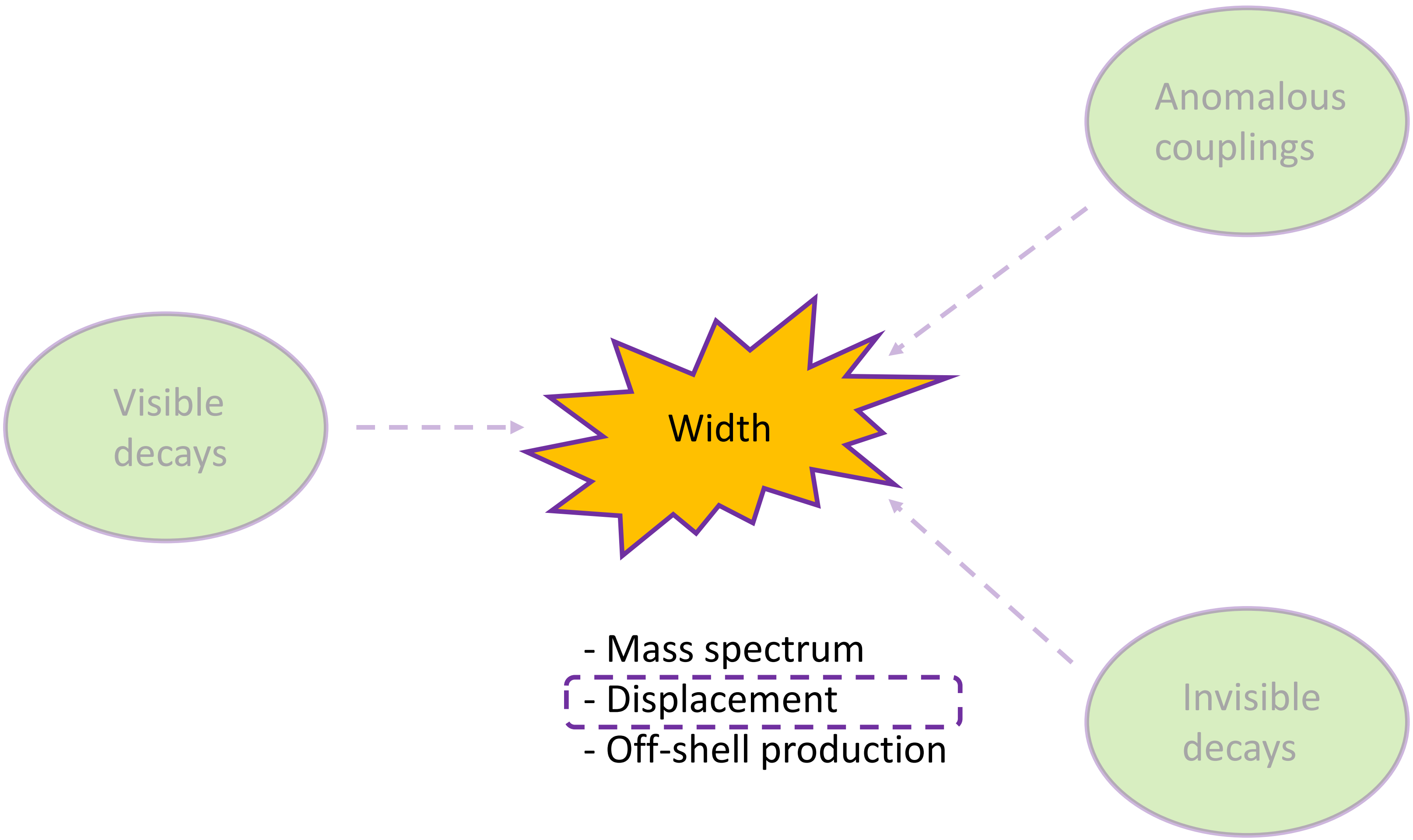

- Mass spectrum
- Displacement
- Off-shell production

SM: 1.6×10^{-22} s
Detector resolution: $\sim 2 \times 10^{-13}$ s

What can we measure?

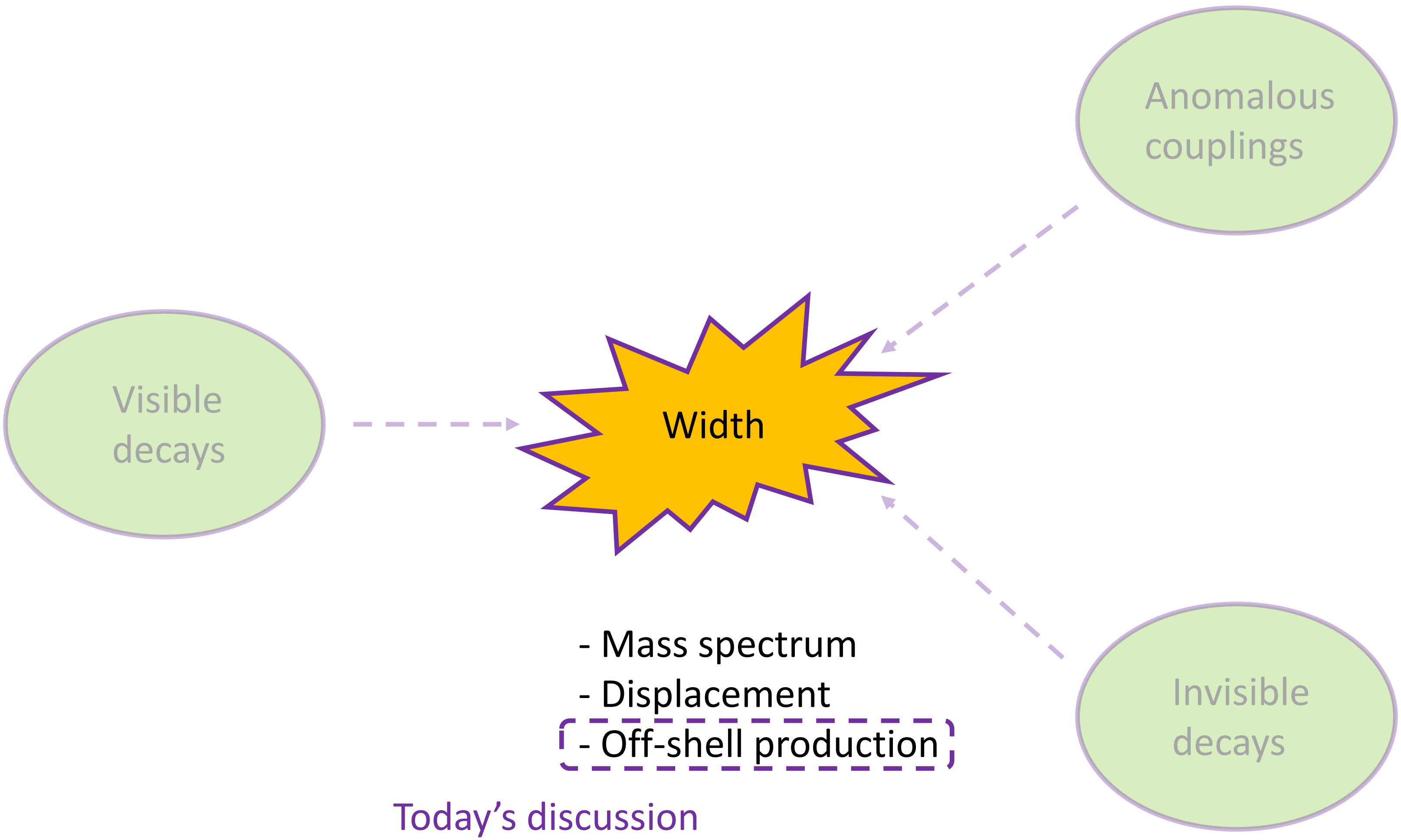

Conventional ways to measure width/lifetime

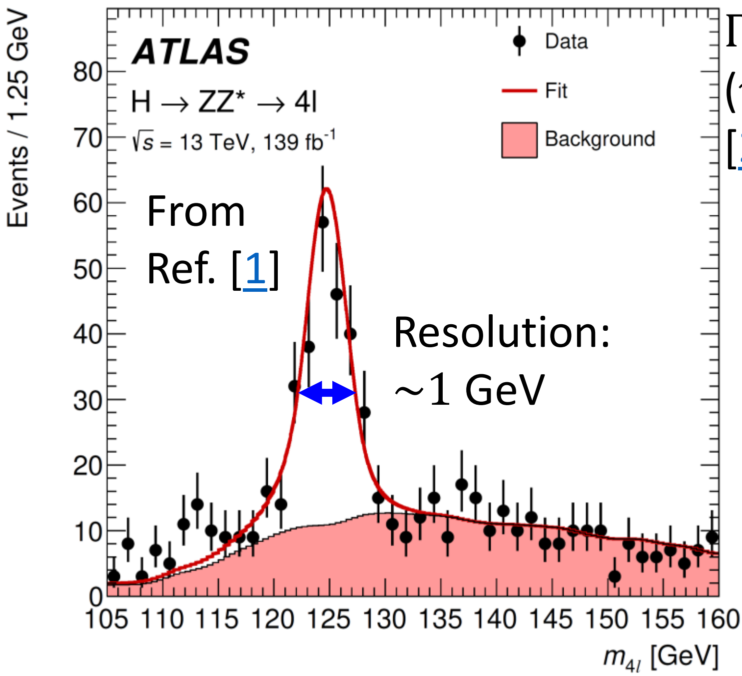

From Ref. [1]

Resolution: $\sim$1 GeV

$\Gamma_{\mathrm{H}} < 1.1$ GeV
($\tau_{\mathrm{H}} > 6.0 \times 10^{-25}$ s)
[2]

$\tau_{\mathrm{H}} < 1.9 \times 10^{-13}$ s
($\Gamma_{\mathrm{H}} > 3.5 \times 10^{-12}$ GeV)
[3]

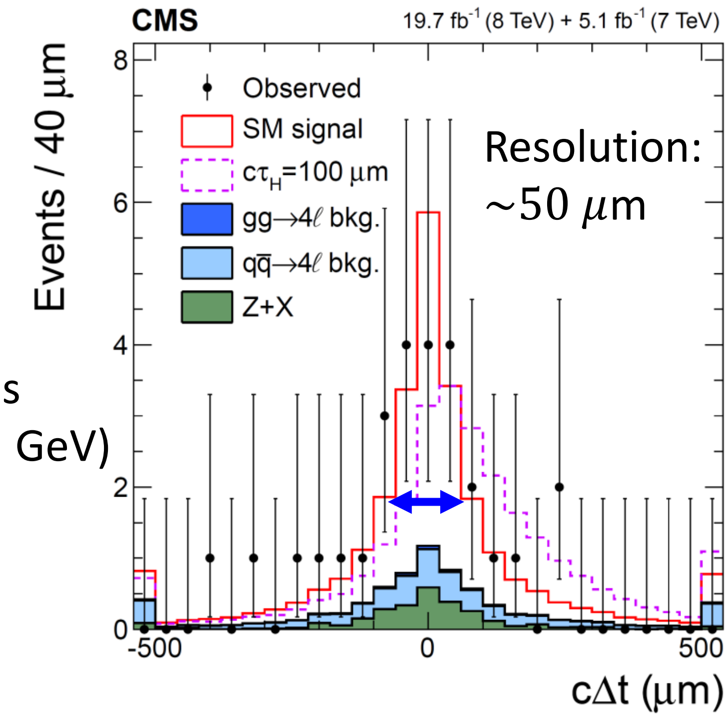

Resolution: $\sim 50\ \mu m$

SM $\Gamma_H = 0.0041$ GeV / $c\tau_H = 4.8 \times 10^{-8}\ \mu m$

[1] ATLAS Collaboration; PLB 843 137880 (2023)
[2] CMS Collaboration; JHEP 11 047 (2017)
[3] CMS Collaboration; PRD 92 072010 (2015)

Conventional ways to measure width/lifetime

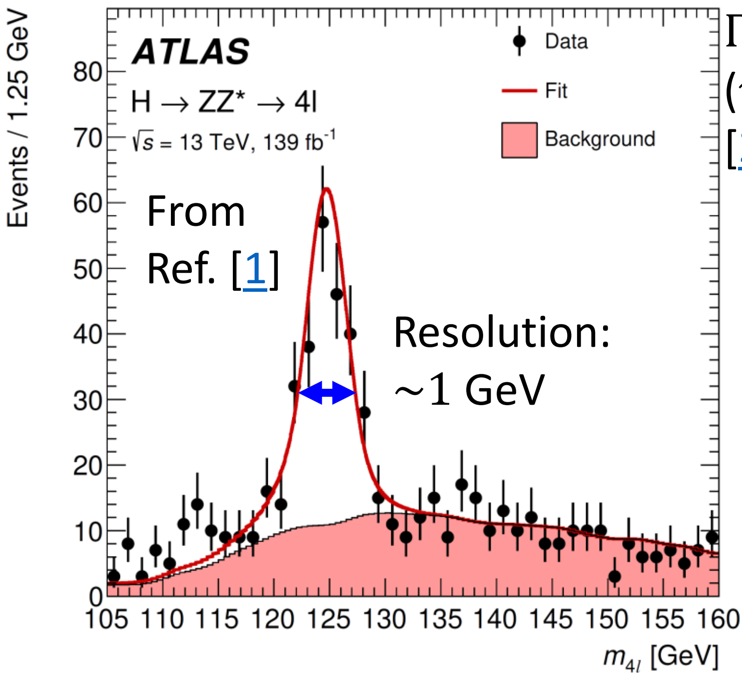

$\Gamma_{\mathrm{H}} < 1.1$ GeV
($\tau_{\mathrm{H}} > 6.0 \times 10^{-25}$ s)
[2]

$\tau_{\mathrm{H}} < 1.9 \times 10^{-13}$ s
($\Gamma_{\mathrm{H}} > 3.5 \times 10^{-12}$ GeV)
[3]

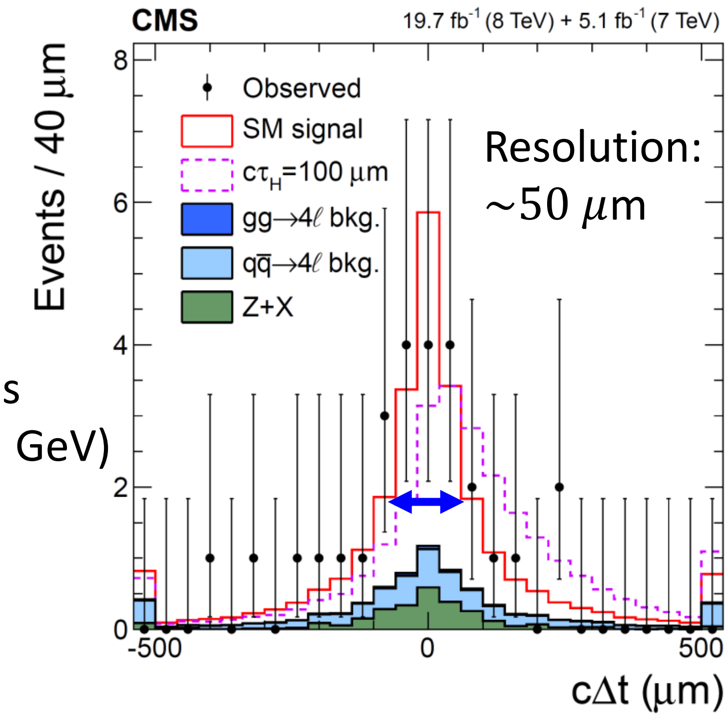

SM $\Gamma_H = 0.0041$ GeV / $c\tau_H = 4.8 \times 10^{-8}\ \mu m$
→ Mass resolution: ~1 GeV
→ 4ℓ vertex resolution: ~50 μm

Γ_H and τ_H too small to be measured directly

[1] ATLAS Collaboration; PLB 843 137880 (2023)
[2] CMS Collaboration; JHEP 11 047 (2017)
[3] CMS Collaboration; PRD 92 072010 (2015)

Off-shell Higgs boson production

In $H \rightarrow VV$ ($V = Z, W$), $m_V < m_{\mathrm{H}} < 2m_V$:
→ On-shell H ($m_{VV} \sim m_H$) ⇒ One off-shell V
→ Off-shell H ($m_{VV} \gg m_H$) ⇒ On-shell Vs

→ Expect $\sim 10\%$ of $H \rightarrow VV$ events in the SM to have an off-shell Higgs boson [1].

Possible to measure two off-shell production mechanisms:
- $\mu_F^{\text{off-shell}}$ (gg)
- $\mu_V^{\text{off-shell}}$ (EW: VBF, VH)
- Can also measure an overall $\mu^{\text{off-shell}}$

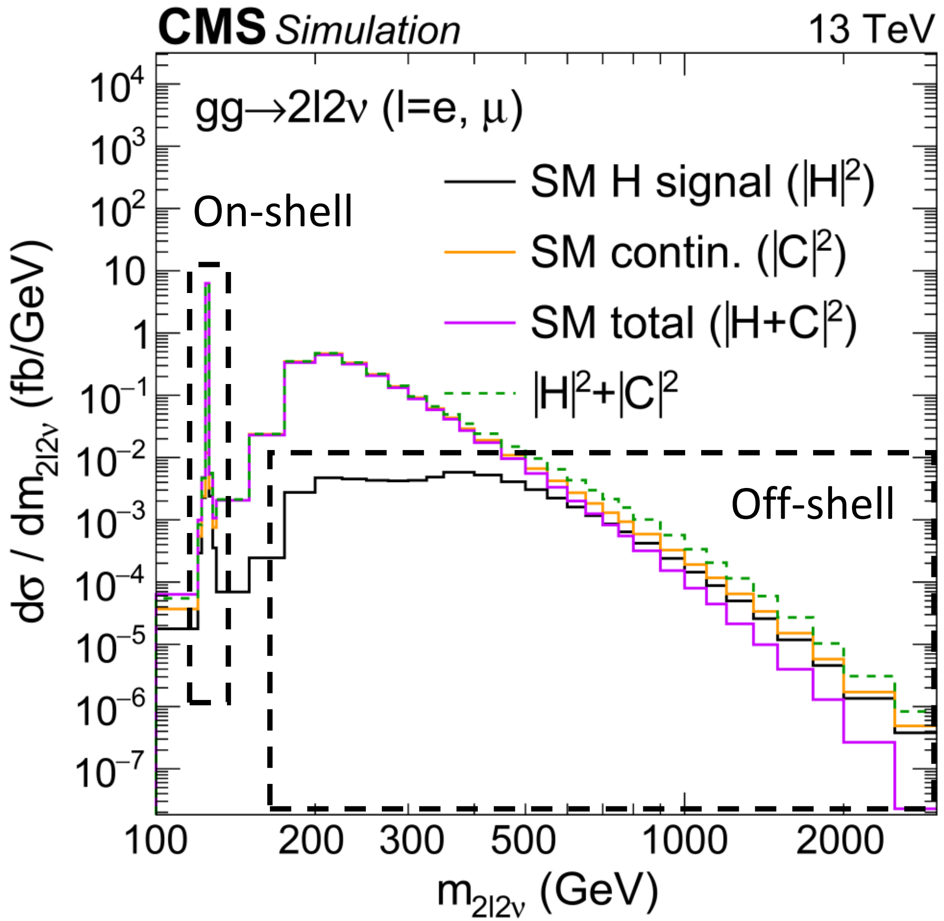

[1] Kauer, N. and Passarino, G.; JHEP 08 116 (2012)

Off-shell Higgs boson production

In $H \rightarrow VV$ ($V = Z, W$), $m_V < m_{\mathrm{H}} < 2m_V$:
→ On-shell H ($m_{VV} \sim m_H$) ⇒ One off-shell V
→ Off-shell H ($m_{VV} \gg m_H$) ⇒ On-shell Vs

→ Expect $\sim 10\%$ of $H \rightarrow VV$ events in the SM to have an off-shell Higgs boson [1].

Possible to measure two off-shell production mechanisms:
- $\mu_F^{\mathrm{off-shell}}$ (gg)
- $\mu_V^{\mathrm{off-shell}}$ (EW: VBF, VH)
- Can also measure an overall $\mu^{\mathrm{off-shell}}$

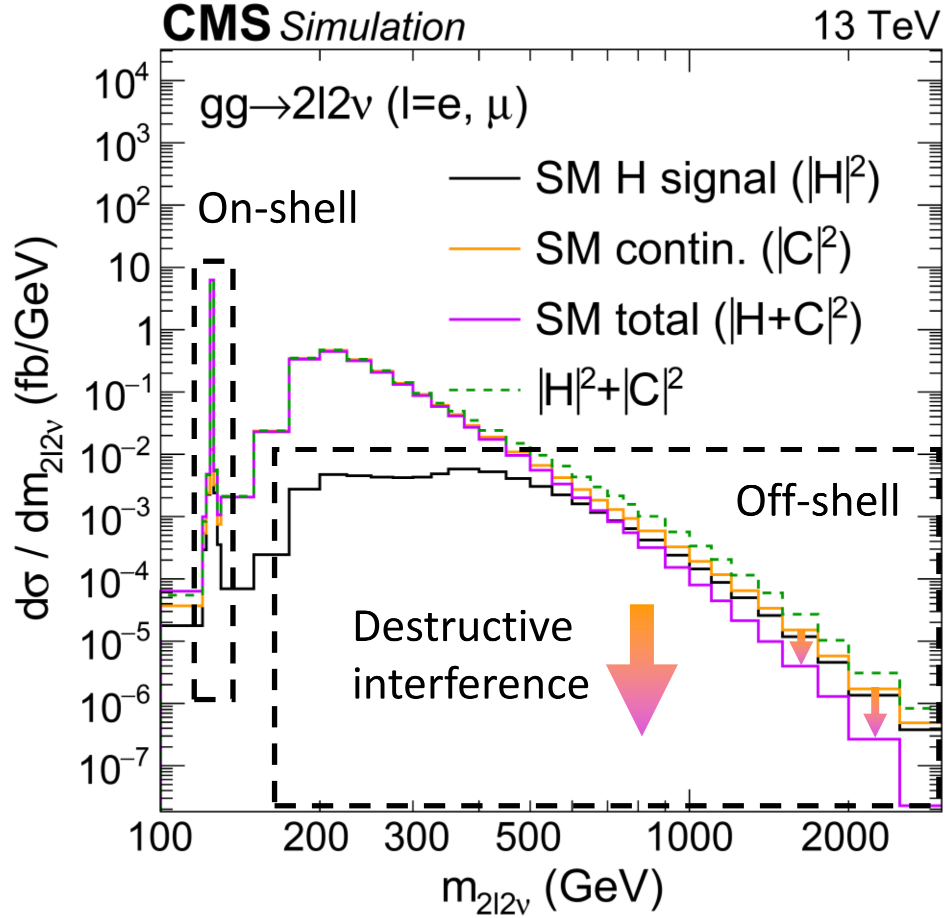

Higgs-mediated diagrams interfere destructively with continuum VV production:
→ Large in magnitude
→ $\sim$Twice the size of the Higgs signal
→ Necessary in the SM to ensure unitarity

[1] Kauer, N. and Passarino, G.; JHEP 08 116 (2012)

Diagrams of off-shell Higgs production

$gg \to H \to ZZ$:

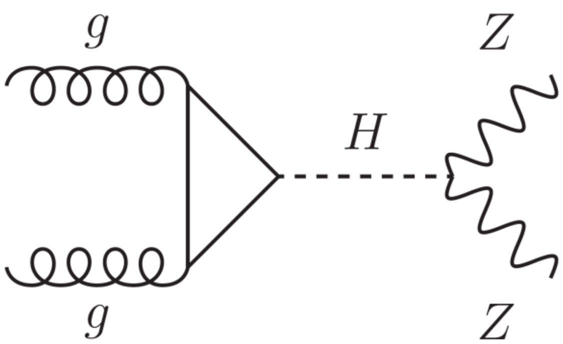

VBF (s-channel):

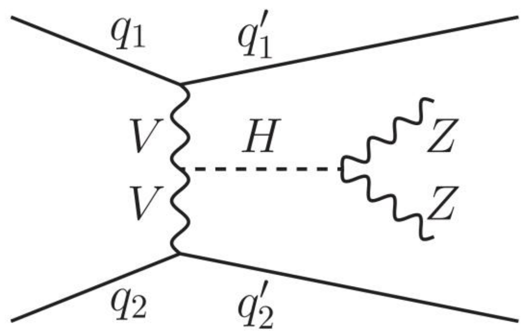

VBF (t-channel):

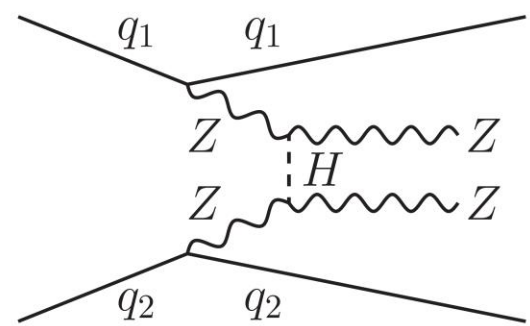

$gg \to H$ production dominant at lower masses in the off-shell region

ZH (s-, t-, u-channels):

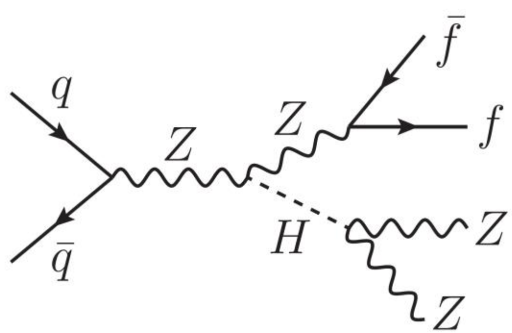

WH:

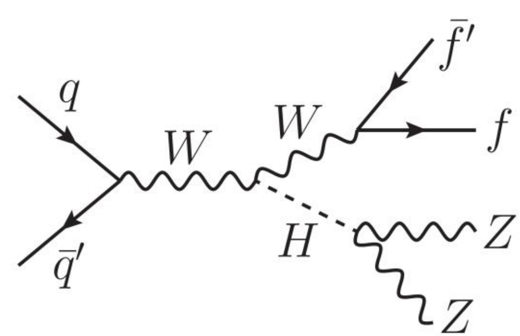

EW production more dominant at higher masses in the off-shell region (mostly VBF in the SM)

Off-shell method for the width

Combine with on-shell signal strength measurement to extract Γ_{H} [1]:

$$\sigma = \int \frac{g_{prod}^2 g_{dec}^2}{(m^2 - m_{\mathrm{H}}^2)^2 + m_{\mathrm{H}}^2 \Gamma_{\mathrm{H}}^2} \ldots dm^2$$

On-shell

$$\sigma \propto \frac{g_{prod}^2 g_{dec}^2}{\Gamma_{\mathrm{H}}} \propto \mu_{prod}$$

Measure on-shell signal strength
from final states ZZ or WW

[1] Caola F. and Melnikov, K. PRD 88 054024 (2013)

Off-shell method for the width

Combine with on-shell signal strength measurement to extract Γ_H [1]:

$$\sigma = \int \frac{g_{prod}^2 g_{dec}^2}{(m^2 - m_\mathrm{H}^2)^2 + m_\mathrm{H}^2 \Gamma_\mathrm{H}^2} \dots dm^2$$

On-shell

Off-shell

$$\sigma \propto \frac{g_{prod}^2 g_{dec}^2}{\Gamma_\mathrm{H}} \propto \mu_{prod}$$

$$\sigma \sim \int \frac{g_{prod}^2 g_{dec}^2}{(m^2 - m_\mathrm{H}^2)^2} \dots dm^2 \propto \mu_{prod}^{\text{off-shell}}$$

Measure on-shell signal strength
from final states ZZ or WW

[1] Caola F. and Melnikov, K.; PRD 88 054024 (2013)

Off-shell method for the width

Combine with on-shell signal strength measurement to extract Γ_{H} [1]:

$$\sigma = \int \frac{g_{prod}^2 g_{dec}^2}{(m^2 - m_{\mathrm{H}}^2)^2 + m_{\mathrm{H}}^2 \Gamma_{\mathrm{H}}^2} \dots dm^2$$

On-shell

$$\sigma \propto \frac{g_{prod}^2 g_{dec}^2}{\Gamma_{\mathrm{H}}} \propto \mu_{prod}$$

Measure on-shell signal strength from final states ZZ or WW

Off-shell

$$\sigma \sim \int \frac{g_{prod}^2 g_{dec}^2}{(m^2 - m_{\mathrm{H}}^2)^2} \dots dm^2 \propto \mu_{prod} \cdot \Gamma_{\mathrm{H}}$$

Ratio of off-shell to on-shell signal strengths for each production mode gives Γ_{H}

[1] Caola F. and Melnikov, K.; PRD 88 054024 (2013)

Off-shell & BSM HVV couplings

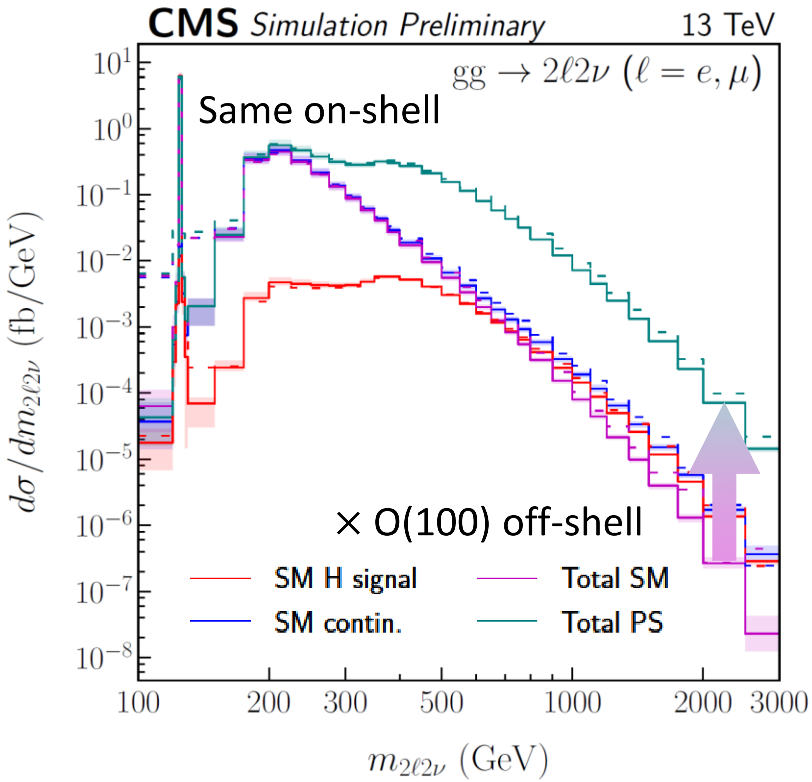

From Ref. [1]

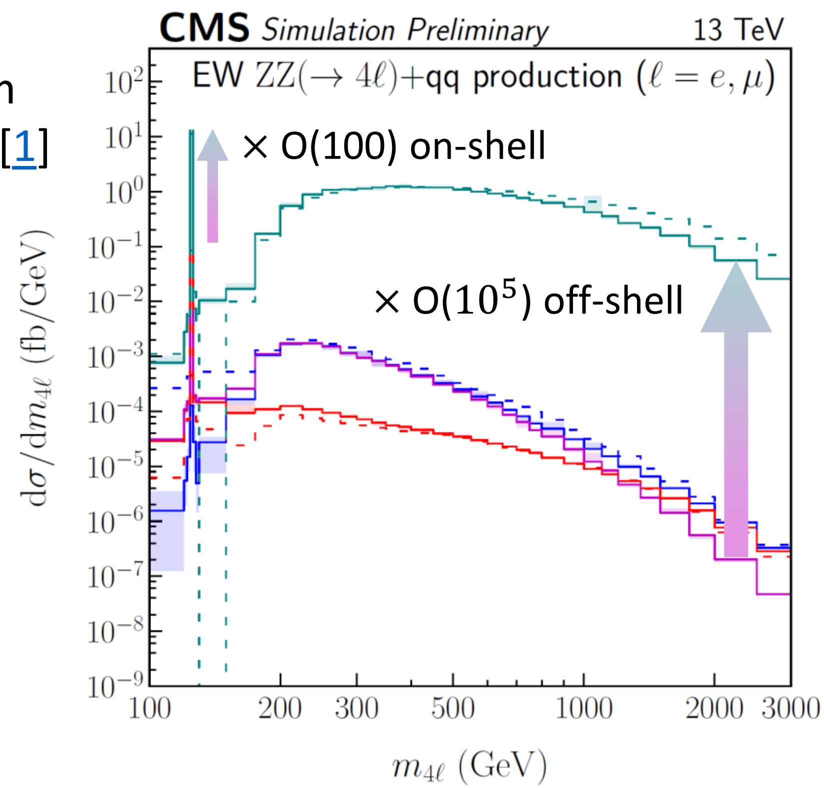

$$A(HVV) \sim \left[a_1 - e^{i\phi_{\Lambda 1}} \frac{(q_{V1}^2 + q_{V2}^2)}{\Lambda_1^2} + \cdots \right] m_V^2 \epsilon_{V1}^* \epsilon_{V2}^*$$
$$+ |a_2|\, e^{i\phi_{a2}}\, f_{\mu\nu}^{*(1)} f^{*(2),\mu\nu} + |a_3|\, e^{i\phi_{a3}}\, f_{\mu\nu}^{*(1)} \tilde{f}^{*(2),\mu\nu}$$

HVV amplitude
$\propto \Lambda_1, a_2, a_3$ BSM contributions
+ SM-like a_1 term

Same a_1 (SM) or a_3 (PS) couplings,
different on-shell and off-shell enhancements
in gg and EW production modes

[1] CMS Collaboration; CMS-NOTE-2022-010, CDS:2826782

We reviewed phenomenology until now.

In what follows, I will focus on the specifics of the $\mathrm{ZZ} \rightarrow 4\ell$ analyses in ATLAS and CMS.

Final results are obtained after combining with $\mathrm{ZZ} \rightarrow 2\ell 2\nu$ and other control regions.

Off-shell 4ℓ: CMS analysis strategy

CMS-HIG-18-002: Analysis of off-shell ($m_{4l} > 220$ GeV) 2016+2017 data [1]
→ All momenta are known in 4ℓ ⇒ Use MELA matrix element discriminants
→ Can compute for Higgs production, decay, or both; or backgrounds

$$\mathcal{D}_{\text{alt}}(\mathbf{\Omega}) = \frac{\mathcal{P}_{\text{sig}}(\mathbf{\Omega})}{\mathcal{P}_{\text{sig}}(\mathbf{\Omega}) + \mathcal{P}_{\text{alt}}(\mathbf{\Omega})}$$

sig. vs alt.

$$\mathcal{D}_{\text{int}}(\mathbf{\Omega}) = \frac{\mathcal{P}_{\text{int}}(\mathbf{\Omega})}{2\sqrt{\mathcal{P}_{\text{sig}}(\mathbf{\Omega})\ \mathcal{P}_{\text{alt}}(\mathbf{\Omega})}}$$

sig.-alt. interference

[1] CMS Collaboration; PRD 99 112003 (2019)

Off-shell 4ℓ: CMS analysis strategy

CMS-HIG-18-002: Analysis of off-shell ($m_{4l} > 220$ GeV) 2016+2017 data [1]

→ All momenta are known in 4ℓ ⇒ Use MELA matrix element discriminants

→ Can compute for Higgs production, decay, or both; or backgrounds

$$\mathcal{D}_{\text{alt}}(\mathbf{\Omega}) = \frac{\mathcal{P}_{\text{sig}}(\mathbf{\Omega})}{\mathcal{P}_{\text{sig}}(\mathbf{\Omega}) + \mathcal{P}_{\text{alt}}(\mathbf{\Omega})}$$

sig. vs alt.

$$\mathcal{D}_{\text{int}}(\mathbf{\Omega}) = \frac{\mathcal{P}_{\text{int}}(\mathbf{\Omega})}{2\sqrt{\mathcal{P}_{\text{sig}}(\mathbf{\Omega})\ \mathcal{P}_{\text{alt}}(\mathbf{\Omega})}}$$

sig.-alt. interference

Category	VBF-tagged	VH-tagged	Untagged
Selection	$\mathcal{D}_{\text{2jet}}^{\text{VBF}}$ or $\mathcal{D}_{\text{2jet}}^{\text{VBF,BSM}} > 0.5$	$\mathcal{D}_{\text{2jet}}^{\text{WH}}$ or $\mathcal{D}_{\text{2jet}}^{\text{WH,BSM}}$, or $\mathcal{D}_{\text{2jet}}^{\text{ZH}}$ or $\mathcal{D}_{\text{2jet}}^{\text{ZH,BSM}} > 0.5$	Rest of events
SM obs.	$m_{4\ell}$, $\mathcal{D}_{\text{bkg}}^{\text{VBF+dec}}$, $\mathcal{D}_{\text{bsi}}^{\text{VBF+dec}}$	$m_{4\ell}$, $\mathcal{D}_{\text{bkg}}^{\text{VH+dec}}$, $\mathcal{D}_{\text{bsi}}^{\text{VH+dec}}$	$m_{4\ell}$, $\mathcal{D}_{\text{bkg}}^{\text{kin}}$, $\mathcal{D}_{\text{bsi}}^{\text{gg,dec}}$

Mass shape is the most sensitive to off-shell production

→ Any off-shell analysis uses a mass-sensitive observable

[1] CMS Collaboration; PRD 99 112003 (2019)

Off-shell 4ℓ: CMS analysis strategy

CMS-HIG-18-002: Analysis of off-shell ($m_{4l} > 220$ GeV) 2016+2017 data [1]
→ All momenta are known in 4ℓ ⇒ Use MELA matrix element discriminants
→ Can compute for Higgs production, decay, or both; or backgrounds

$$\mathcal{D}_{\mathrm{alt}}(\boldsymbol{\Omega}) = \frac{\mathcal{P}_{\mathrm{sig}}(\boldsymbol{\Omega})}{\mathcal{P}_{\mathrm{sig}}(\boldsymbol{\Omega}) + \mathcal{P}_{\mathrm{alt}}(\boldsymbol{\Omega})}$$

sig. vs alt.

$$\mathcal{D}_{\mathrm{int}}(\boldsymbol{\Omega}) = \frac{\mathcal{P}_{\mathrm{int}}(\boldsymbol{\Omega})}{2\sqrt{\mathcal{P}_{\mathrm{sig}}(\boldsymbol{\Omega})\ \mathcal{P}_{\mathrm{alt}}(\boldsymbol{\Omega})}}$$

sig.-alt. interference

Category	VBF-tagged	VH-tagged	Untagged
Selection	$\mathcal{D}_{\mathrm{2jet}}^{\mathrm{VBF}}$ or $\mathcal{D}_{\mathrm{2jet}}^{\mathrm{VBF,BSM}} > 0.5$	$\mathcal{D}_{\mathrm{2jet}}^{\mathrm{WH}}$ or $\mathcal{D}_{\mathrm{2jet}}^{\mathrm{WH,BSM}}$, or $\mathcal{D}_{\mathrm{2jet}}^{\mathrm{ZH}}$ or $\mathcal{D}_{\mathrm{2jet}}^{\mathrm{ZH,BSM}} > 0.5$	Rest of events
SM obs.	$m_{4\ell}$, $\mathcal{D}_{\mathrm{bkg}}^{\mathrm{VBF+dec}}$, $\mathcal{D}_{\mathrm{bsi}}^{\mathrm{VBF+dec}}$	$m_{4\ell}$, $\mathcal{D}_{\mathrm{bkg}}^{\mathrm{VH+dec}}$, $\mathcal{D}_{\mathrm{bsi}}^{\mathrm{VH+dec}}$	$m_{4\ell}$, $\mathcal{D}_{\mathrm{bkg}}^{\mathrm{kin}}$, $\mathcal{D}_{\mathrm{bsi}}^{\mathrm{gg,dec}}$

Mass shape is the most sensitive to off-shell production
→ Any off-shell analysis uses a mass-sensitive observable

+ Discriminant for signal vs bkg
+ Discriminant for Higgs-continuum ZZ interference
  (or SM vs BSM if constraining anomalous couplings)

[1] CMS Collaboration; PRD 99 112003 (2019)

Off-shell 4ℓ: CMS event distributions

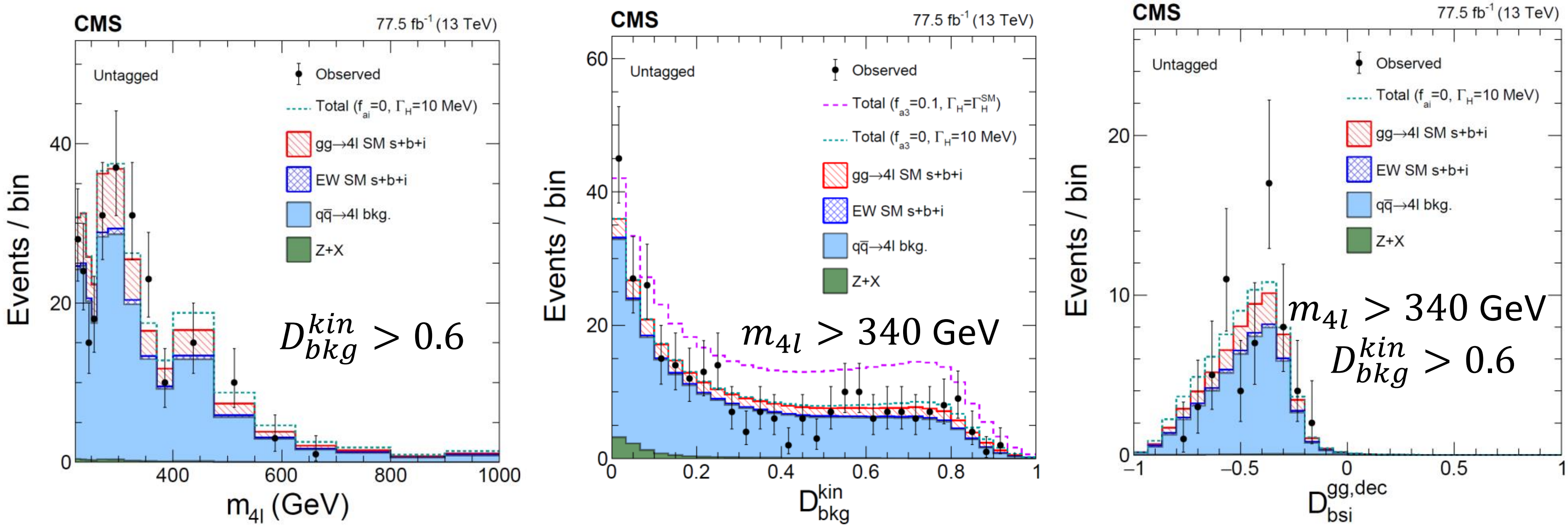

Example distributions from the untagged category

Selection requirements are applied on the plots
to enhance Higgs contributions

Stacked histograms for prefit SM distributions ($\Gamma_{\mathrm{H}} = 4.1$ MeV),
cyan for $\Gamma_{\mathrm{H}} = 10$ MeV, magenta for an on-shell 10% PS (a_3) mixture

[1] CMS Collaboration; PRD 99 112003 (2019)

Off-shell 4ℓ: ATLAS analysis

ATLAS-HIGG-2018-32: Analysis of off-shell ($m_{4l} > 220$ GeV) 2016-2018 data, with $m_{4l} \in (180, 220)$ GeV used to constraint $q\bar{q} \to ZZ$ [1]
→ Event selection follows Ref. [2] closely.

[1] ATLAS Collaboration; arxiv:2304.01532 (2023)
[2] ATLAS Collaboration; EPJC 81 332 (2021)

Off-shell 4ℓ: ATLAS analysis

ATLAS-HIGG-2018-32: Analysis of off-shell ($m_{4l} > 220$ GeV) 2016-2018 data, with $m_{4l} \in (180, 220)$ GeV used to constraint $q\bar{q} \rightarrow ZZ$ [1]

→ Event selection follows Ref. [2] closely.

→ Categorization depends on the number of jets ($p_{\mathrm{T}} > 30$ GeV, $|\eta| < 4.5$):

- EW signal region: $N_j \geq 2$ and $|\Delta\eta_{jj}| > 4$ (~46% of Higgs prod. EW)
- 1-jet mixed signal region: $N_j = 1$ and $|\eta_j| > 2.5$ (~5% of Higgs prod. EW)
- ggF signal region: All other events ($\sim$6% of Higgs prod. EW)

[1] ATLAS Collaboration; arxiv:2304.01532 (2023)
[2] ATLAS Collaboration; EPJC 81 332 (2021)

Off-shell 4ℓ: ATLAS analysis

ATLAS-HIGG-2018-32: Analysis of off-shell ($m_{4l} > 220$ GeV) 2016-2018 data, with $m_{4l} \in (180, 220)$ GeV used to constraint $q\bar{q} \to ZZ$ [1]
→ Event selection follows Ref. [2] closely.
→ Observables include information on the invariant mass.

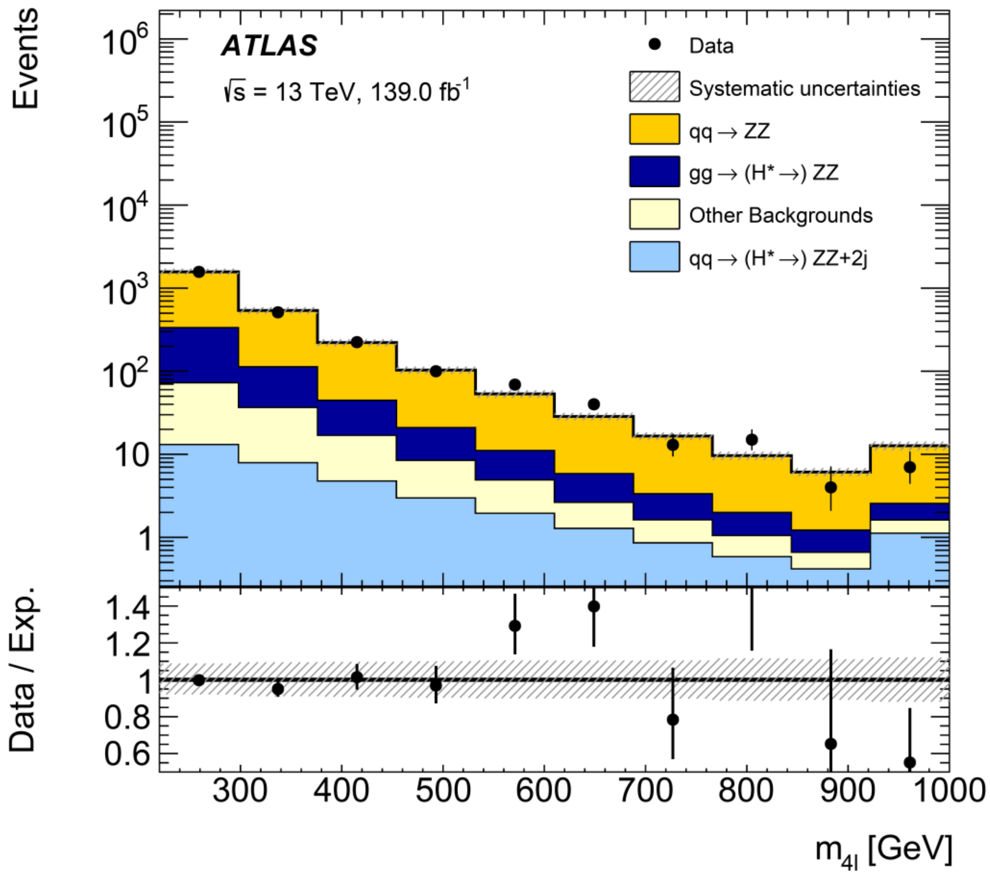

Postfit distribution w/ $\mu^{\text{off-shell}} = 1$

[1] ATLAS Collaboration; arxiv:2304.01532 (2023)
[2] ATLAS Collaboration; EPJC 81 332 (2021)

Off-shell 4ℓ: ATLAS analysis

ATLAS-HIGG-2018-32: Analysis of off-shell ($m_{4l} > 220$ GeV) 2016-2018 data, with $m_{4l} \in (180, 220)$ GeV used to constraint $q\bar{q} \to ZZ$ [1]

→ Event selection follows Ref. [2] closely.

→ Observables include NN discriminants with the following general form:

$$\mathcal{O}_{NN} = \log_{10} \frac{P_S}{P_B}$$

- P_S: ggF or EW Higgs production processes
- P_B: Interfering and noninterfering bkgs. (input as two separate classes)

→ $\mathcal{O}_{\text{ggF}}$ ($\mathcal{O}_{\text{EW}}$) used in the ggF and mixed (EW) SRs

[1] ATLAS Collaboration; arxiv:2304.01532 (2023)

[2] ATLAS Collaboration; EPJC 81 332 (2021)

Off-shell 4ℓ: ATLAS analysis

ATLAS-HIGG-2018-32: Analysis of off-shell ($m_{4l} > 220$ GeV) 2016-2018 data, with $m_{4l} \in (180, 220)$ GeV used to constraint $q\bar{q} \to ZZ$ [1]

→ Event selection follows Ref. [2] closely.

→ $\mathcal{O}_{\mathrm{ggF}}$ ($\mathcal{O}_{\mathrm{EW}}$) used in the ggF and mixed (EW) SRs

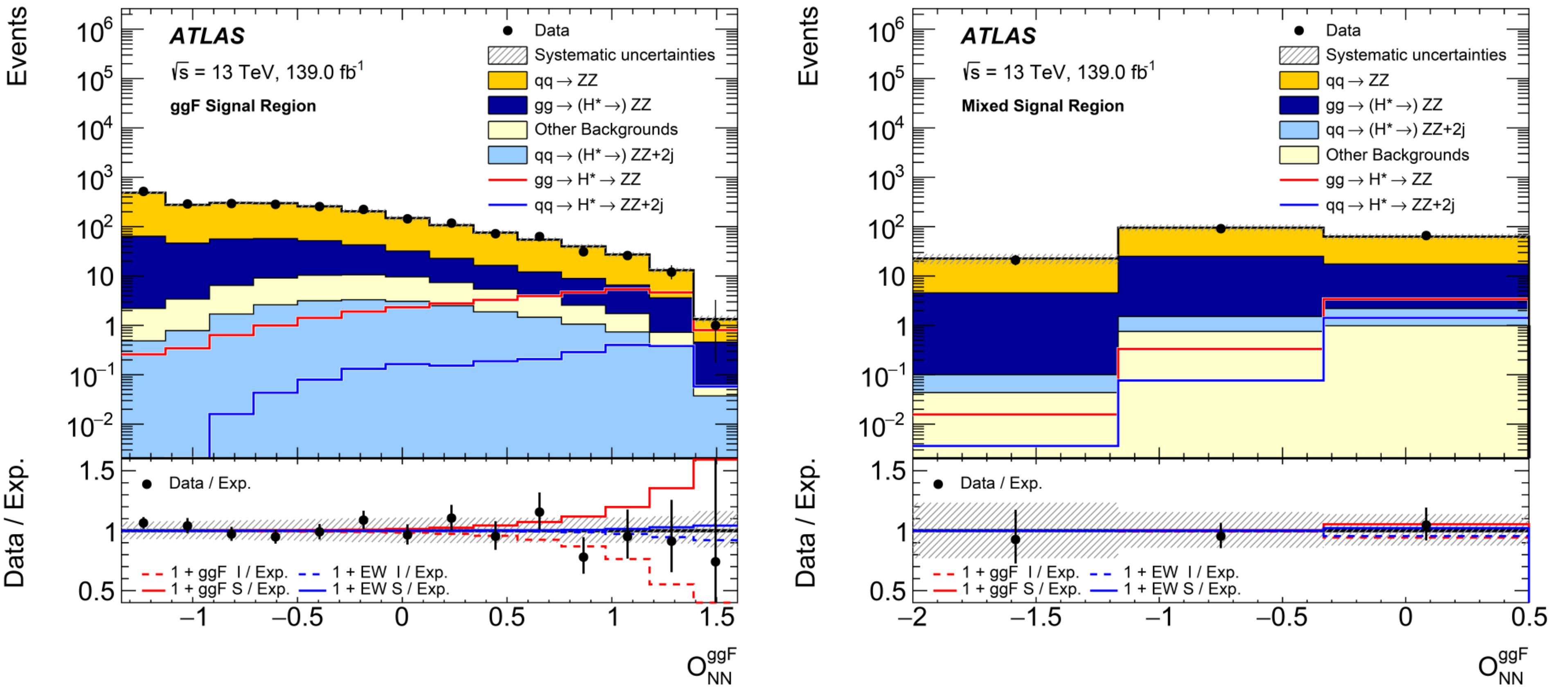

[1] ATLAS Collaboration; arxiv:2304.01532 (2023)

[2] ATLAS Collaboration; EPJC 81 332 (2021)

Off-shell 4ℓ: ATLAS analysis

ATLAS-HIGG-2018-32: Analysis of off-shell ($m_{4l} > 220$ GeV) 2016-2018 data, with $m_{4l} \in (180, 220)$ GeV used to constraint $q\bar{q} \to ZZ$ [1]
→ Event selection follows Ref. [2] closely.
→ $\mathcal{O}_{\mathrm{ggF}}$ ($\mathcal{O}_{\mathrm{EW}}$) used in the ggF and mixed (EW) SRs

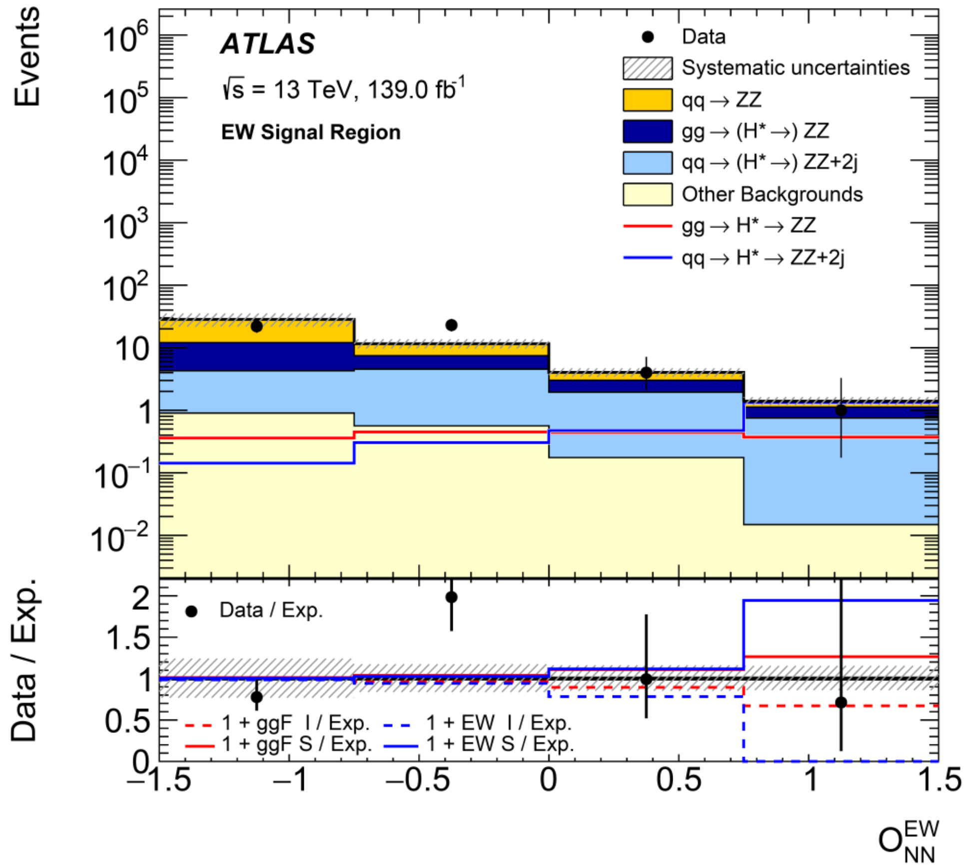

[1] ATLAS Collaboration; arxiv:2304.01532 (2023)
[2] ATLAS Collaboration; EPJC 81 332 (2021)

On-shell 4ℓ: CMS analysis

CMS-HIG-19-009: Analysis of on-shell 4ℓ 2016-2018 data [1]
→ Utilizes a finer categorization and more discriminants as observables
→ Same categorization and observables for all couplings
→ Example from untagged category:

$$\mathcal{D}_{\rm bkg}, \mathcal{D}^{\rm dec}_{0h+}, \mathcal{D}^{\rm dec}_{0-}, \mathcal{D}^{\rm dec}_{\Lambda1}, \mathcal{D}^{Z\gamma,\rm dec}_{\Lambda1}, \mathcal{D}^{\rm dec}_{\rm int}, \mathcal{D}^{\rm dec}_{CP}$$

SM vs BSM — SM-BSM interf.

Provides extensive set of results
→ Provides the following input to off-shell analysis:
on-shell μ_F and μ_V
on-shell BSM HVV contribution fractions f_{ai}

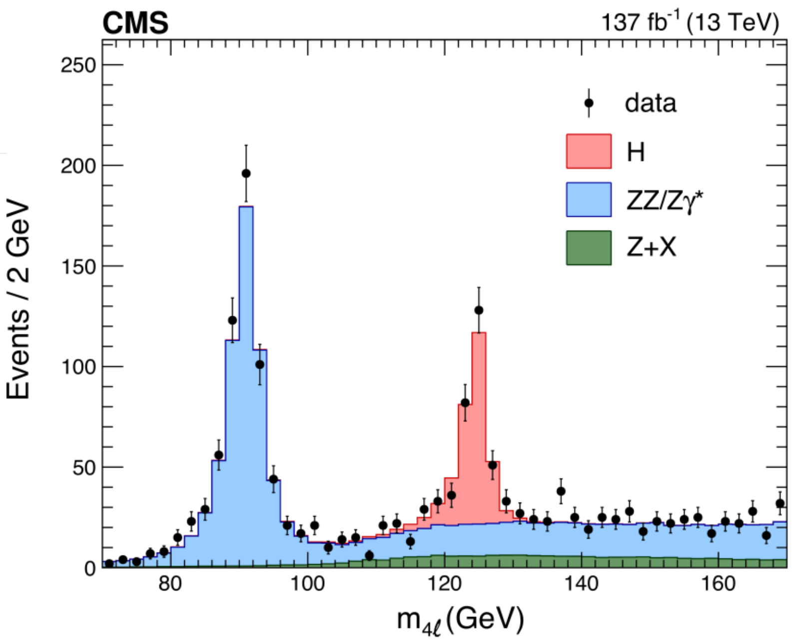

[1] CMS Collaboration; PRD 104 052004 (2021)

On-shell 4ℓ: CMS analysis

CMS-HIG-19-009: Analysis of on-shell 4ℓ 2016-2018 data [1]

→ Utilizes a finer categorization and more discriminants as observables

→ Same categorization and observables for all couplings

→ Example from untagged category:

$$\mathcal{D}_{\text{bkg}}, \mathcal{D}_{0h+}^{\text{dec}}, \mathcal{D}_{0-}^{\text{dec}}, \mathcal{D}_{\Lambda1}^{\text{dec}}, \mathcal{D}_{\Lambda1}^{Z\gamma,\text{dec}}, \mathcal{D}_{\text{int}}^{\text{dec}}, \mathcal{D}_{CP}^{\text{dec}}$$

SM vs BSM SM-BSM interf.

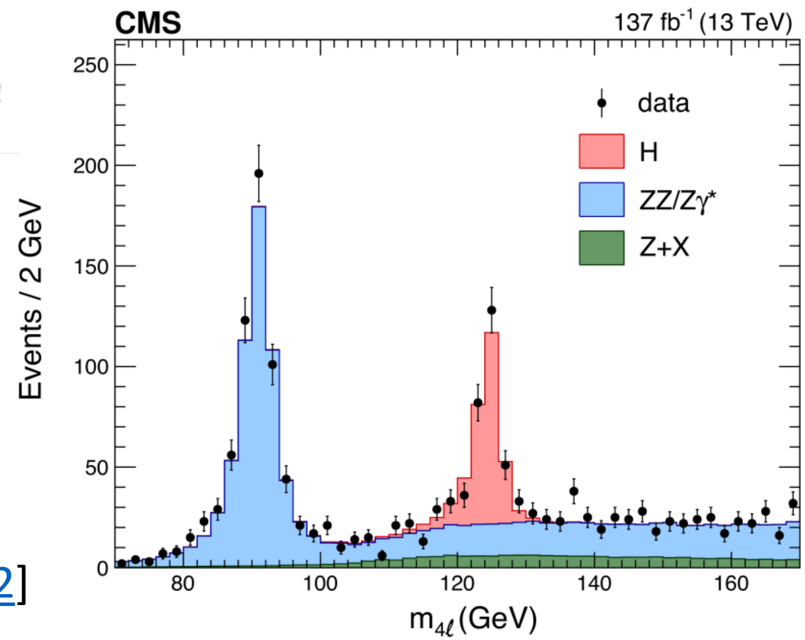

Provides extensive set of results

→ Provides the following input to off-shell analysis:

on-shell μ_F and μ_V

on-shell BSM HVV contribution fractions f_{ai}

CMS-HIG-17-011: Analysis of on-shell 4ℓ 2015 data [2]

→ Inclusive in categorization

→ Observables: $D_{bkg}, D_{BSM}^{dec}, D_{int}^{dec}$ as in the untagged category above.

→ The BSM discriminant depends on the analyzed coupling.

[1] CMS Collaboration; PRD 104 052004 (2021)

[2] CMS Collaboration; PLB 775 1 (2017)

On-shell 4ℓ: ATLAS analysis

ATLAS-HIGG-2018-28: Analysis of on-shell 4ℓ 2016-2018 data [1]
→ On-shell region as $m_{4\ell} \in (115, 130)$ GeV w/ sideband 105 - 160 GeV outside this range
→ See backup for full event selection reqs.

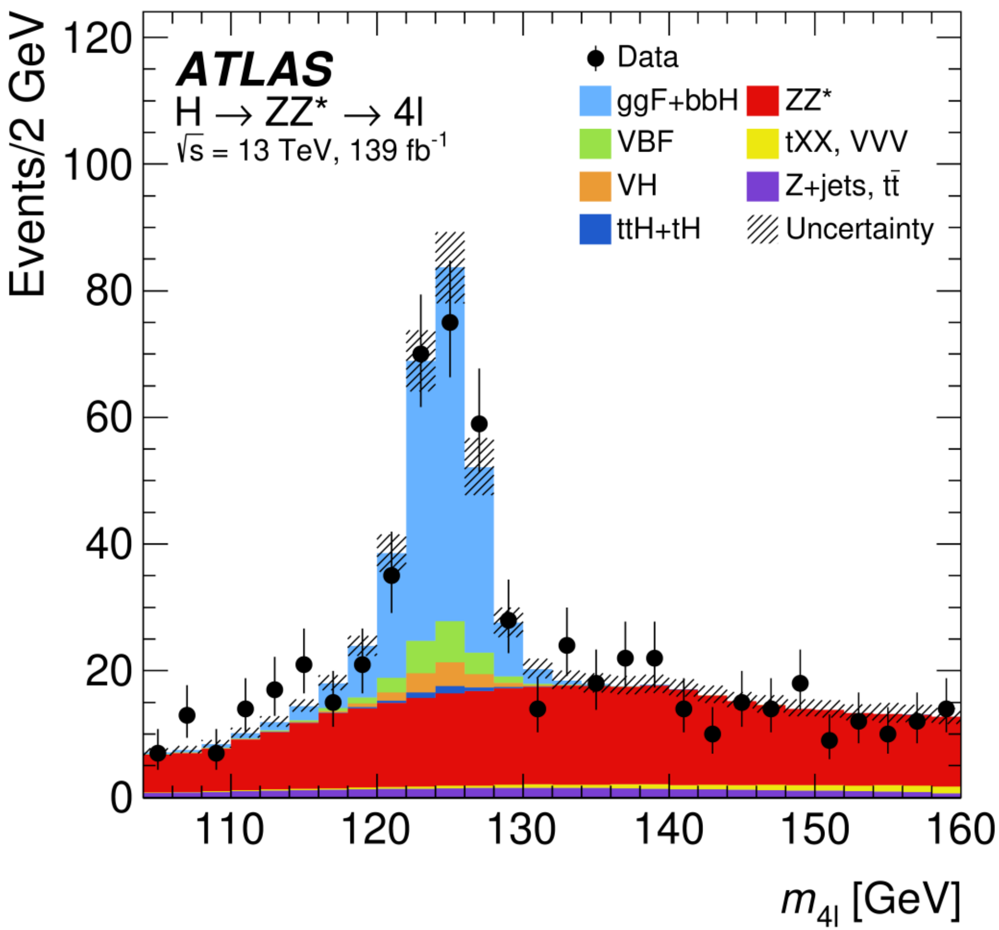

Postfit distribution
w/ $m_H = 125$ GeV

[1] ATLAS Collaboration; EPJC 80 957 (2020)
Errata: EPJC 81 29 (2021), EPJC 81 398 (2021)

On-shell 4ℓ: ATLAS analysis

ATLAS-HIGG-2018-28: Analysis of on-shell 4ℓ 2016-2018 data [1]
→ On-shell region as $m_{4\ell} \in (115, 130)$ GeV w/ sideband 105 - 160 GeV outside this range
→ See backup for full event selection reqs.
→ STXS-style event categorization and discriminants

Category	Processes	MLP	Lepton RNN	Jet RNN	Discriminant
$0j$-$p_T^{4\ell}$-Low $0j$-$p_T^{4\ell}$-Med	ggF, ZZ^*	$p_T^{4\ell}$, D_{ZZ^*}, m_{12}, m_{34}, $\lvert\cos\theta^*\rvert$, $\cos\theta_1$, ϕ_{ZZ}	p_T^ℓ, η_ℓ	-	NN_{ggF}
$1j$-$p_T^{4\ell}$-Low	ggF, VBF, ZZ^*	$p_T^{4\ell}$, p_T^j, η_j, $\Delta R_{4\ell j}$, D_{ZZ^*}	p_T^ℓ, η_ℓ	-	NN_{VBF} for $\text{NN}_{ZZ} < 0.25$ NN_{ZZ} for $\text{NN}_{ZZ} > 0.25$
$1j$-$p_T^{4\ell}$-Med	ggF, VBF, ZZ^*	$p_T^{4\ell}$, p_T^j, η_j, E_T^{miss}, $\Delta R_{4\ell j}$, D_{ZZ^*}, $\eta_{4\ell}$	p_T^ℓ, η_ℓ	-	NN_{VBF} for $\text{NN}_{ZZ} < 0.25$ NN_{ZZ} for $\text{NN}_{ZZ} > 0.25$
$1j$-$p_T^{4\ell}$-High	ggF, VBF	$p_T^{4\ell}$, p_T^j, η_j, E_T^{miss}, $\Delta R_{4\ell j}$, $\eta_{4\ell}$	p_T^ℓ, η_ℓ	-	NN_{VBF}
$2j$	ggF, VBF, VH	m_{jj}, $p_T^{4\ell jj}$	p_T^ℓ, η_ℓ	p_T^j, η_j	NN_{VBF} for $\text{NN}_{VH} < 0.2$ NN_{VH} for $\text{NN}_{VH} > 0.2$
$2j$-BSM-like	ggF, VBF	η_{ZZ}^{Zepp}, $p_T^{4\ell jj}$	p_T^ℓ, η_ℓ	p_T^j, η_j	NN_{VBF}
VH-Lep-enriched	VH, ttH	N_{jets}, $N_{b\text{-jets},70\%}$, E_T^{miss}, H_T	p_T^ℓ	-	NN_{ttH}
ttH-Had-enriched	ggF, ttH, tXX	$p_T^{4\ell}$, m_{jj}, $\Delta R_{4\ell j}$, $N_{b\text{-jets},70\%}$,	p_T^ℓ, η_ℓ	p_T^j, η_j	NN_{ttH} for $\text{NN}_{tXX} < 0.4$ NN_{tXX} for $\text{NN}_{tXX} > 0.4$

[1] ATLAS Collaboration; EPJC 80 957 (2020)
Errata: EPJC 81 29 (2021), EPJC 81 398 (2021)

CMS results

Evidence for off-shell from $2\ell2\nu + 4\ell$

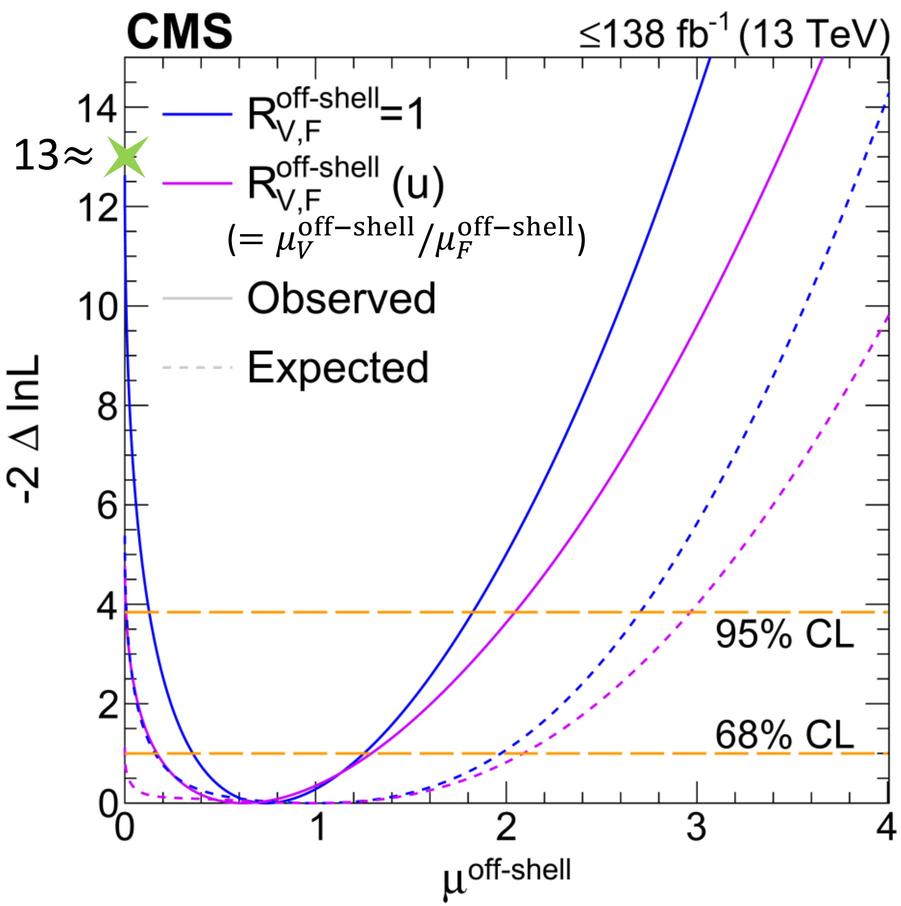

No – off-shell scenario ($\mu^{\text{off-shell}} = 0$) is excluded at p=0.0003 (3.6 std. devs.)
→ Using asymptotic approximation, validated with Neyman construction (toys) at $\mu = 0$, and 68/95% CL

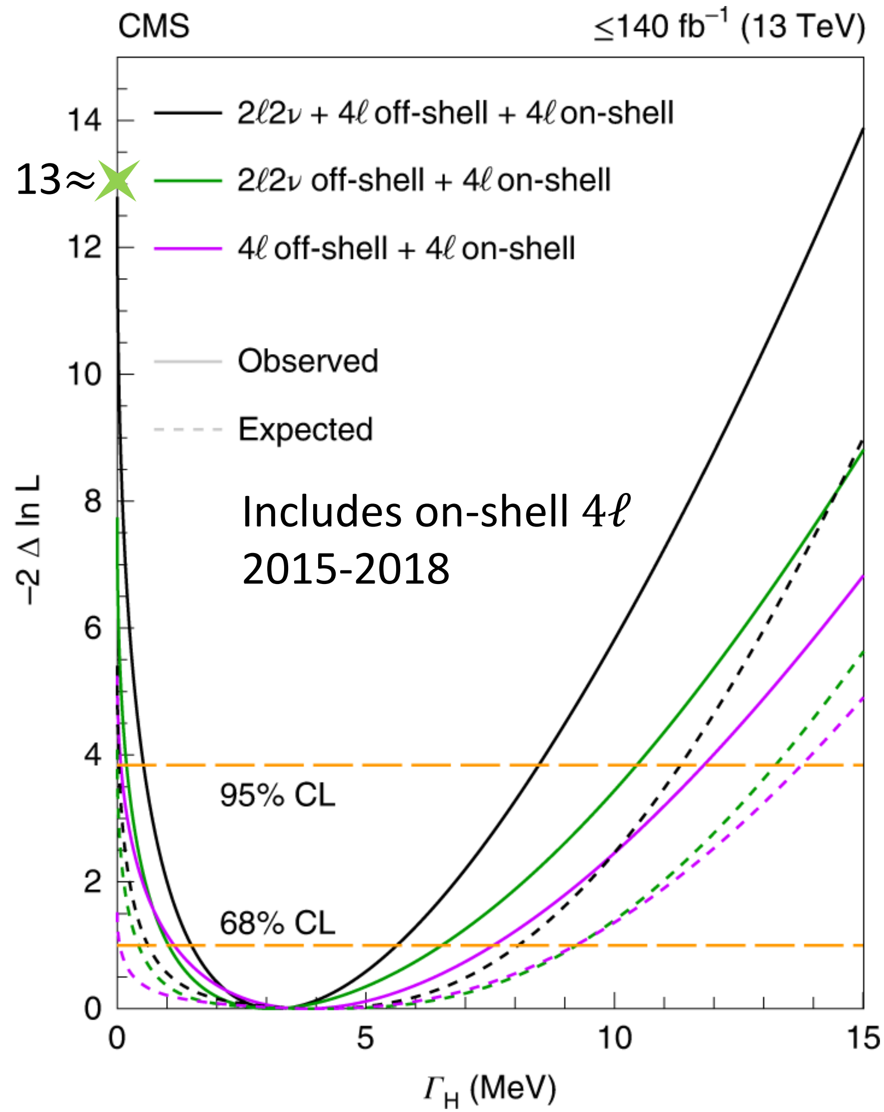

Observed $\Gamma_H = 3.2^{+2.4}_{-1.7}$ MeV
[0.5, 8.5] MeV @ 95% CL

[1] CMS Collaboration; Nature Phys. 18 11 (2022)

$\mu_F^{\text{off-shell}}$ and $\mu_V^{\text{off-shell}}$

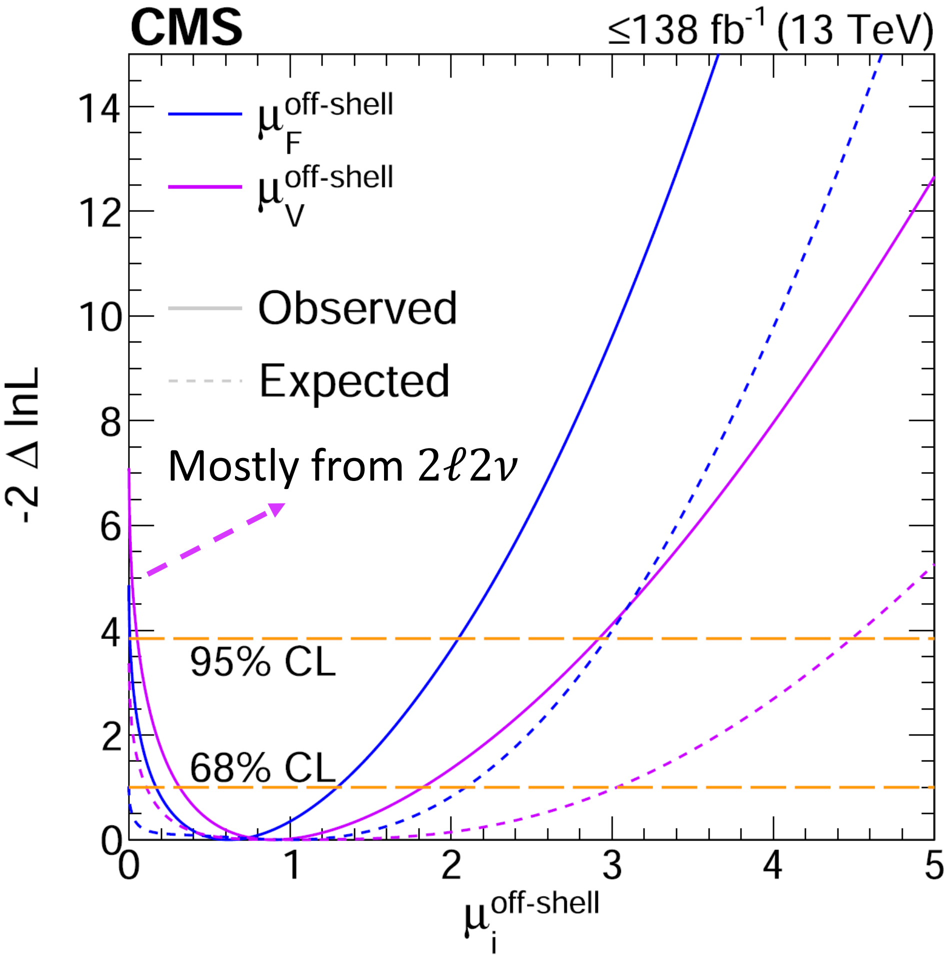

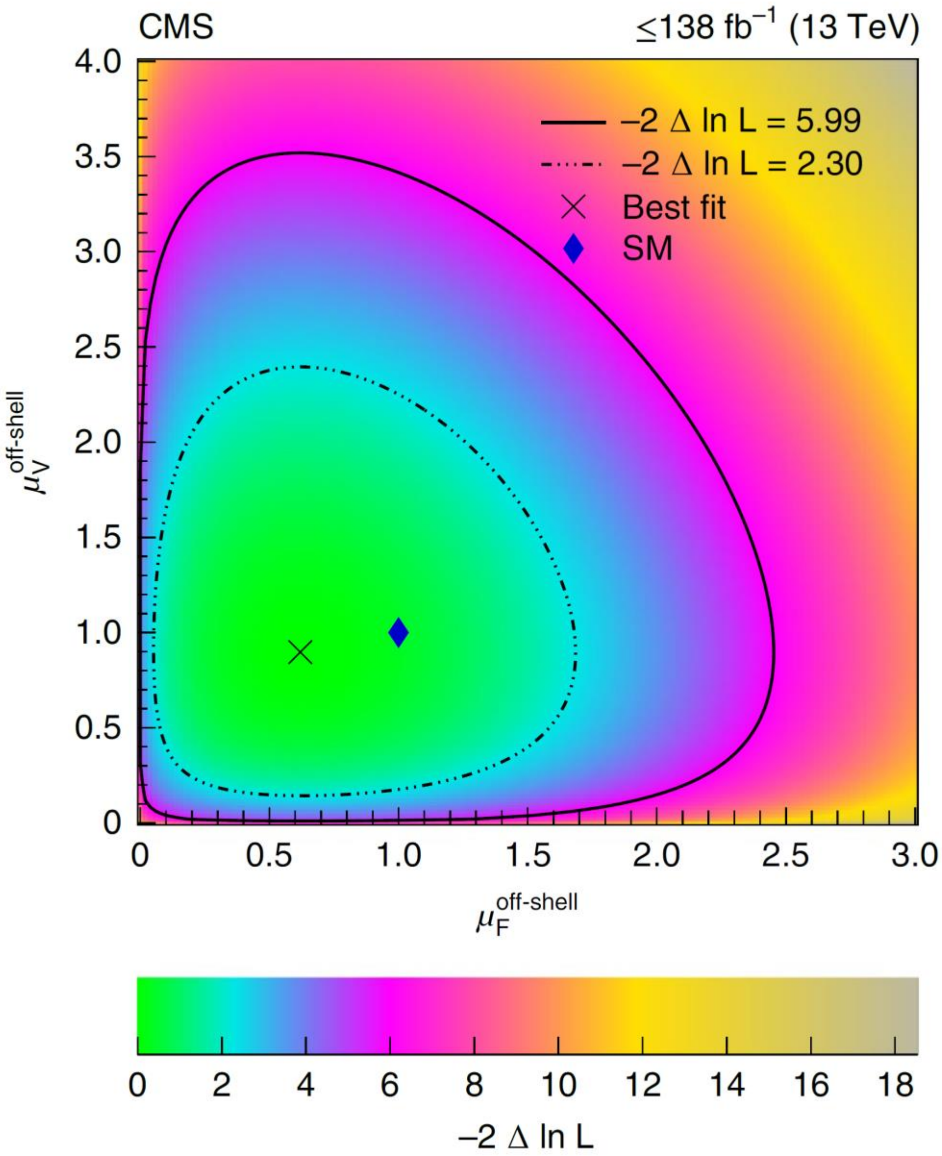

Joint constraints on
$\mu_F^{\text{off-shell}}$ (gg production) and
$\mu_V^{\text{off-shell}}$ (EW production)

[1] CMS Collaboration; Nature Phys. 18 11 (2022)

Anomalous HVV couplings from off-shell

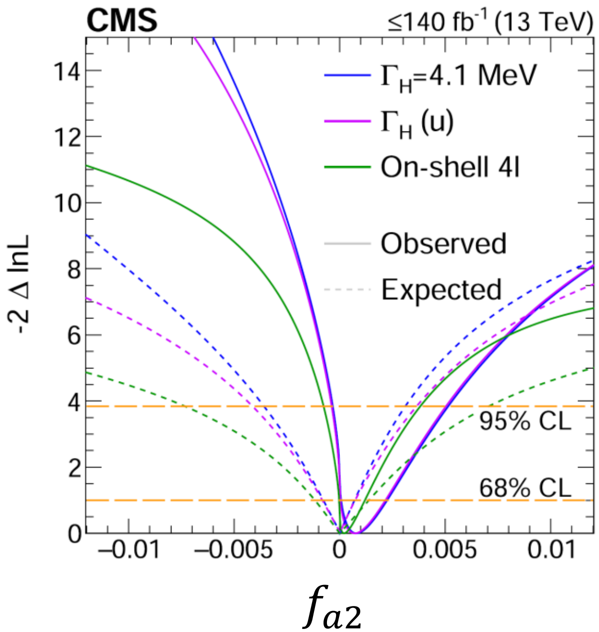

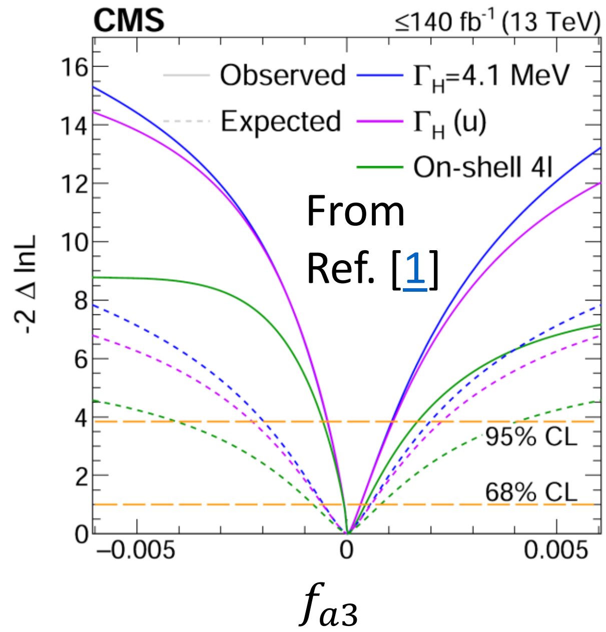

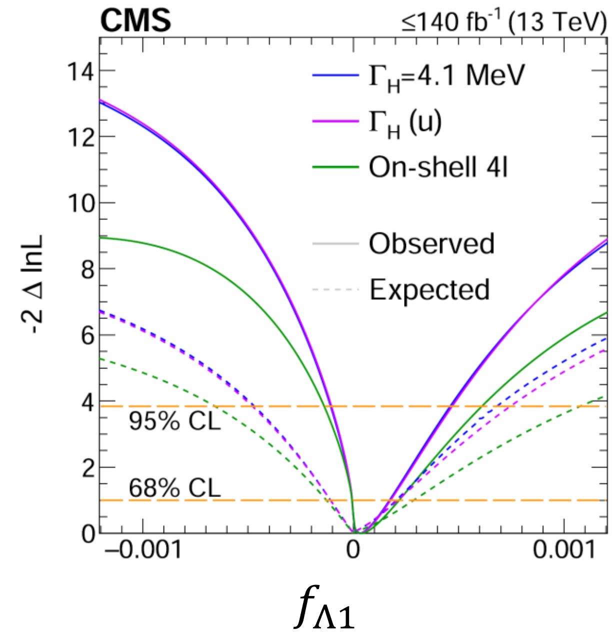

O(10^{-5}–10^{-3}) constraints on fractional BSM contributions

O(10%) improvement from adding off-shell information

Other on-shell - only measurements [2] constrain these couplings even further.

[1] CMS Collaboration; Nature Phys. 18 11 (2022)
[2] CMS Collaboration; arxiv:2205.05120 (2022)

Anomalous HVV couplings from off-shell

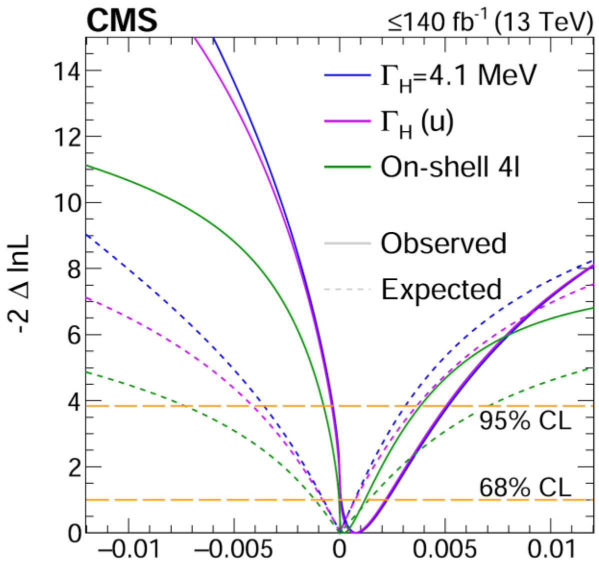

f_{a2}

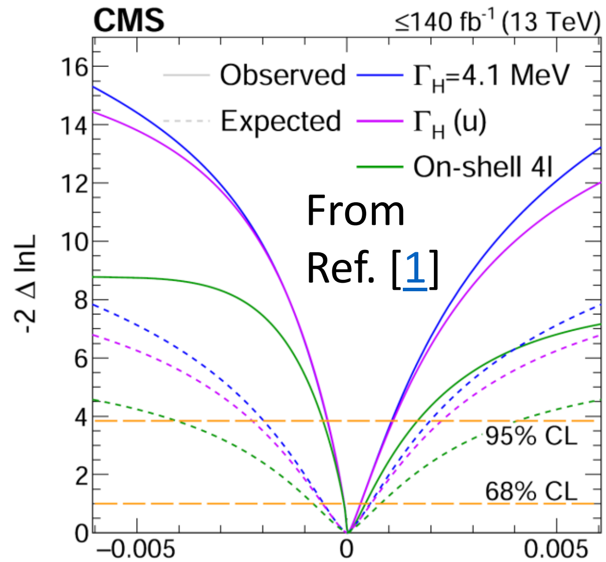

f_{a3}

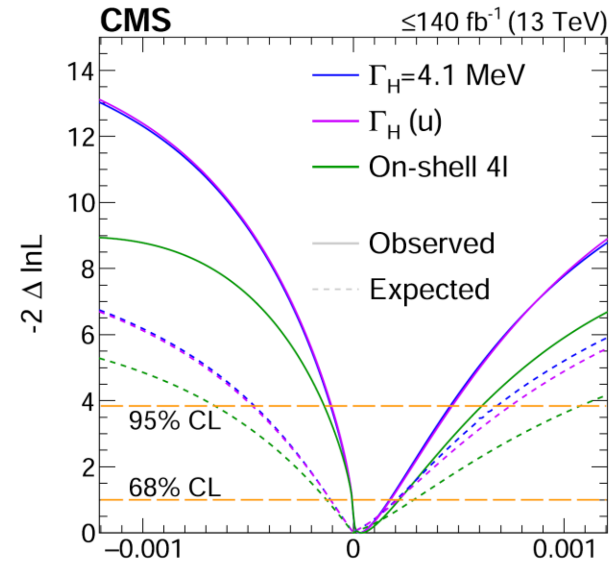

$f_{\Lambda 1}$

Measurement of the width stable when testing different anomalous HVV couplings

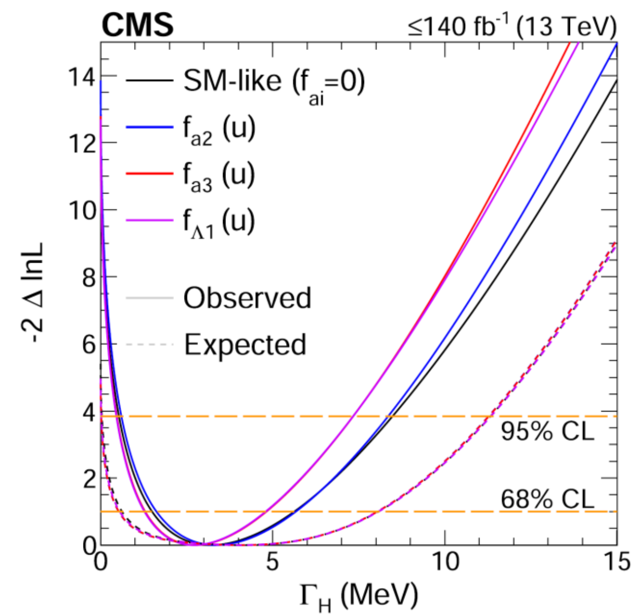

[1] CMS Collaboration; Nature Phys. 18 11 (2022)

ATLAS results

Evidence for off-shell from $2\ell 2\nu + 4\ell$

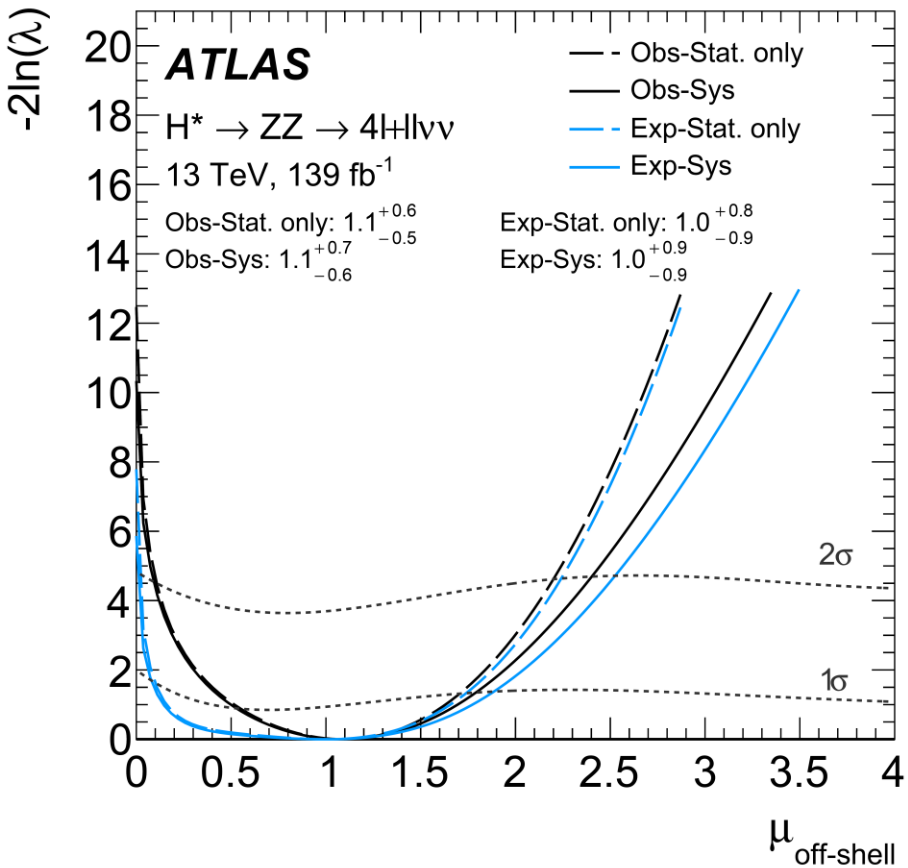

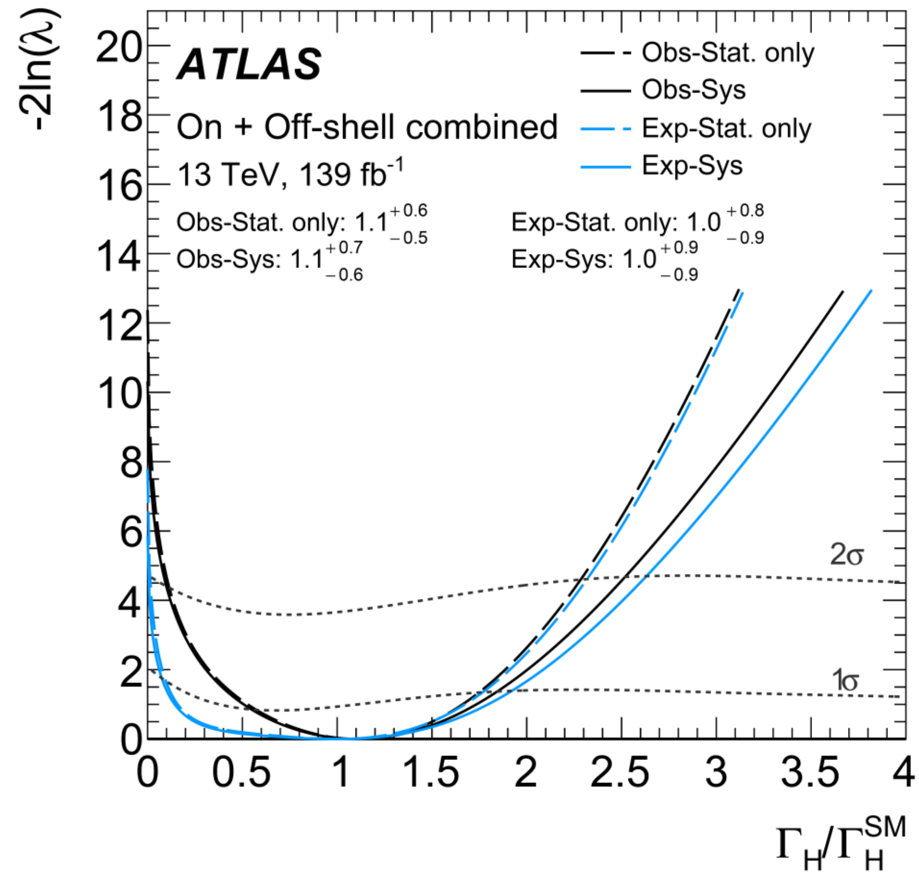

No – off-shell scenario ($\mu^{\text{off}-\text{shell}} = 0$) is excluded at 3.2 std. devs.
→ Note that dotted curves on the left are for Neyman construction (toys)

Observed $\Gamma_{\text{H}} = 4.5^{+3.3}_{-2.5}$ MeV
[0.5, 10.5] MeV @ 95% CL

[1] ATLAS Collaboration; arxiv:2304.01532 (2023)

$\mu_{\text{off-shell}}^{\text{ggF}}$ and $\mu_{\text{off-shell}}^{\text{EW}}$

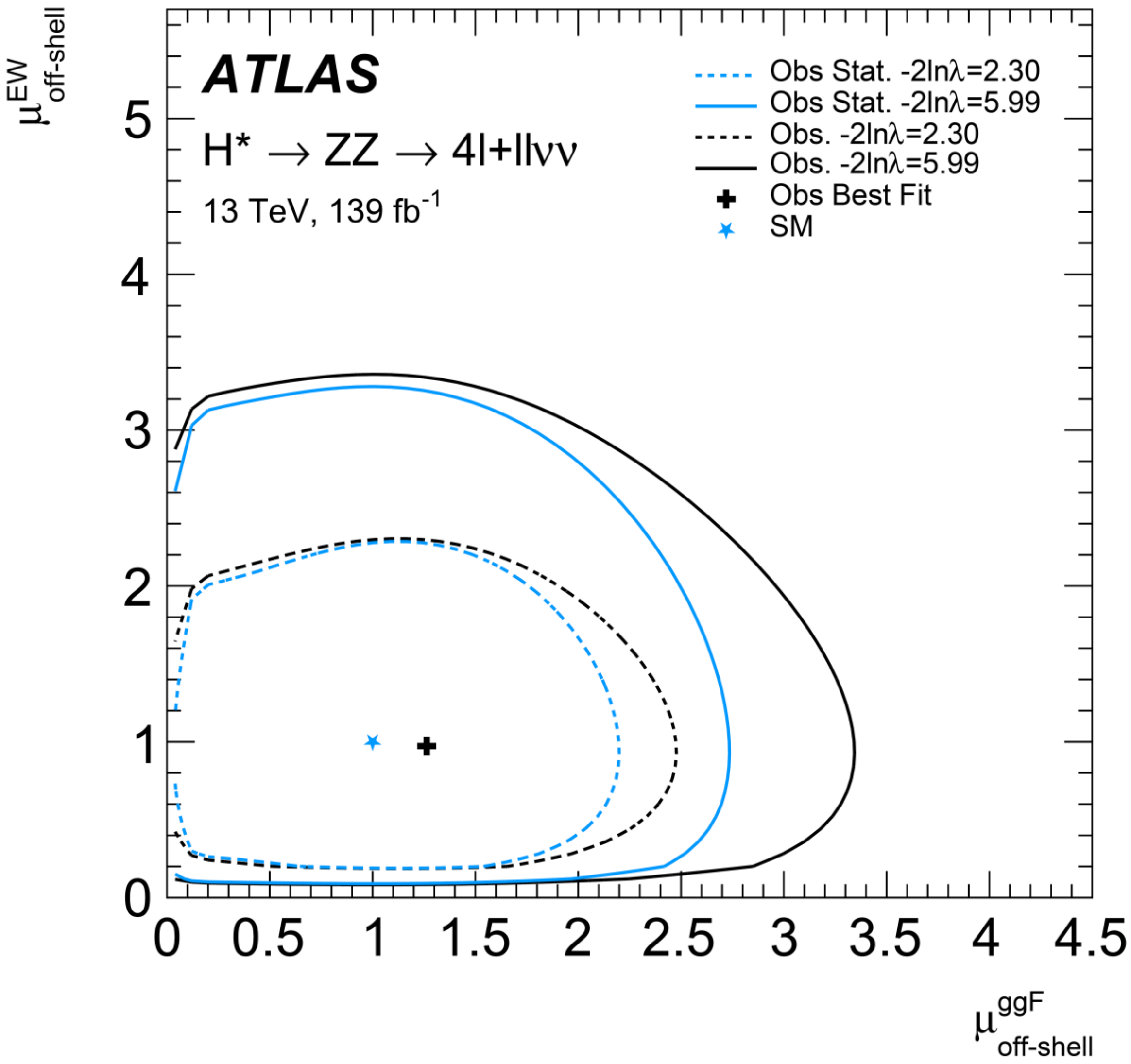

Joint constraints on $\mu_{\text{off-shell}}^{\text{ggF}}$ and $\mu_{\text{off-shell}}^{\text{EW}}$

Result in agreement with CMS and the SM

[1] ATLAS Collaboration; arxiv:2304.01532 (2023)

R_{gg} and R_{VV}

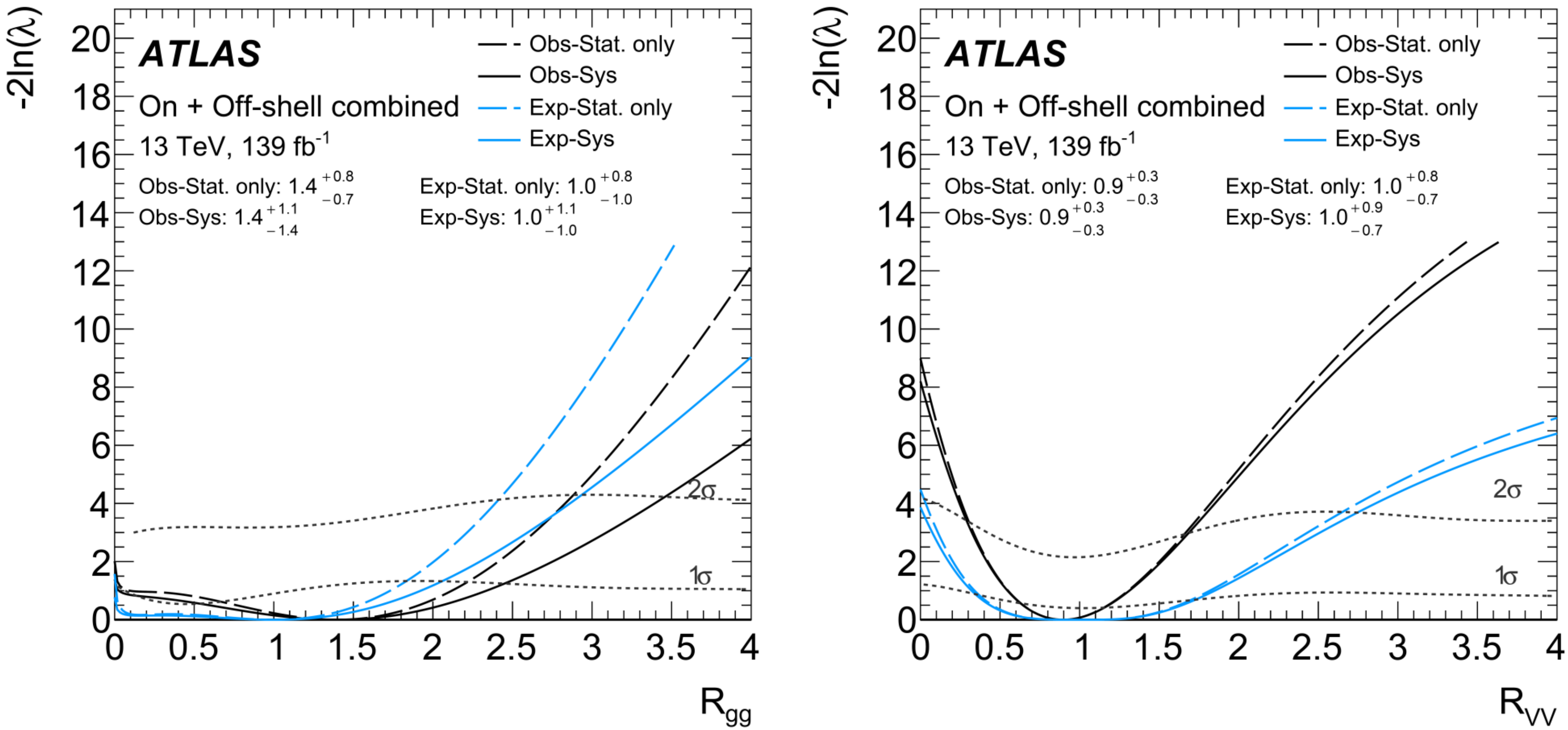

Results also interpreted in terms of off-shell/on-shell coupling multipliers, w/ $\Gamma_{\mathrm{H}} = 4.1$ MeV:

→ $R_{gg} = \kappa^2_{g,\mathrm{off-shell}} \,/\, \kappa^2_{g,\mathrm{on-shell}}$ and $R_{VV} = \kappa^2_{V,\mathrm{off-shell}} \,/\, \kappa^2_{V,\mathrm{on-shell}}$

→ Results consistent with the SM

[1] ATLAS Collaboration; arxiv:2304.01532 (2023)

Summary

Presented the current status of the off-shell analysis in CMS and ATLAS:
→ Off-shell Higgs production in VV final states Important in the SM for unitarity
→ Combination with on-shell information can allow us to measure the total width
  → Large deviations can hint at BSM couplings to the Higgs boson

→ Analysis consists of 4ℓ off-shell and on-shell, and $2\ell 2\nu$ off-shell components
  → Particular emphasis is given today on the 4ℓ analyses
  → Additional information on other components can be found in the references.

→ Evidence for off-shell Higgs boson contributions in the $\mathrm{ZZ} \to 4\ell + 2\ell 2\nu$ final state from both CMS and ATLAS!

→ Total width measurements consistent with the SM value of $\Gamma_{\mathrm{H}} = 4.1$ MeV
  → Additional interpretations considering anomalous HVV couplings or different off-shell/on-shell coupling multiplier relations considered - no significant devs. from the SM

Stay tuned for more exciting results as we continue to collect data in Run 3 and develop analysis methods further!

References

Theory:

Caola F. and Melnikov, K.; PRD 88 054024 (2013)
Kauer, N. and Passarino, G.; JHEP 08 116 (2012)

CMS:

CMS-NOTE-2022-010, CDS:2826782
Nature Phys. 18 11 (2022)
arxiv:2205.05120 (2022)
PRD 104 052004 (2021)
PRD 99 112003 (2019)
JHEP 11 047 (2017)
PLB 775 1 (2017)
PRD 92 072010 (2015)

ATLAS:

arxiv:2304.01532 (2023)
PLB 843 137880 (2023)
EPJC 81 332 (2021)
EPJC 80 957 (2020) w/ errata:
EPJC 81 398 (2021) and EPJC 81 29 (2021)

Additional materials:

LHC Higgs Off-shell Subgroup; CDS:2801789 (2022)
SMEFiT Collaboration; JHEP 11 089 (2021)
Sarica, U. Springer Theses (2019)
LHC Higgs WG; CERN-2017-002-M
Caola, F. et al.; JHEP 07 087 (2016)

Back-up

Typical lepton efficiencies

Detector is very efficient in reconstructing leptons.
→ Here are exemplary lepton selection efficiencies.

Muons: ~85% – 98%

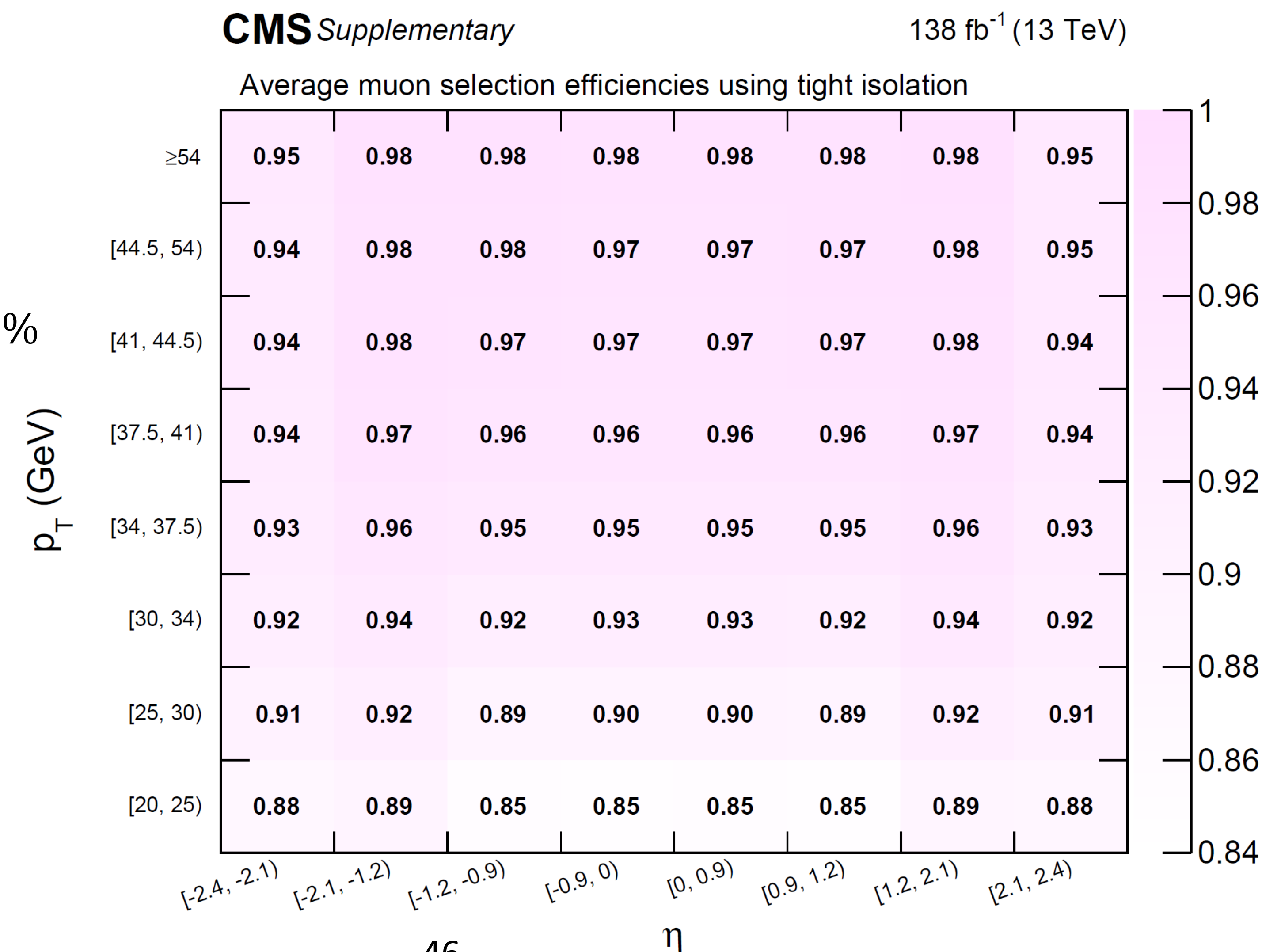

Typical lepton efficiencies

Detector is very efficient in reconstructing leptons.
→ Here are exemplary lepton selection efficiencies.

Electrons: $\sim 48\% \; - 88\%$

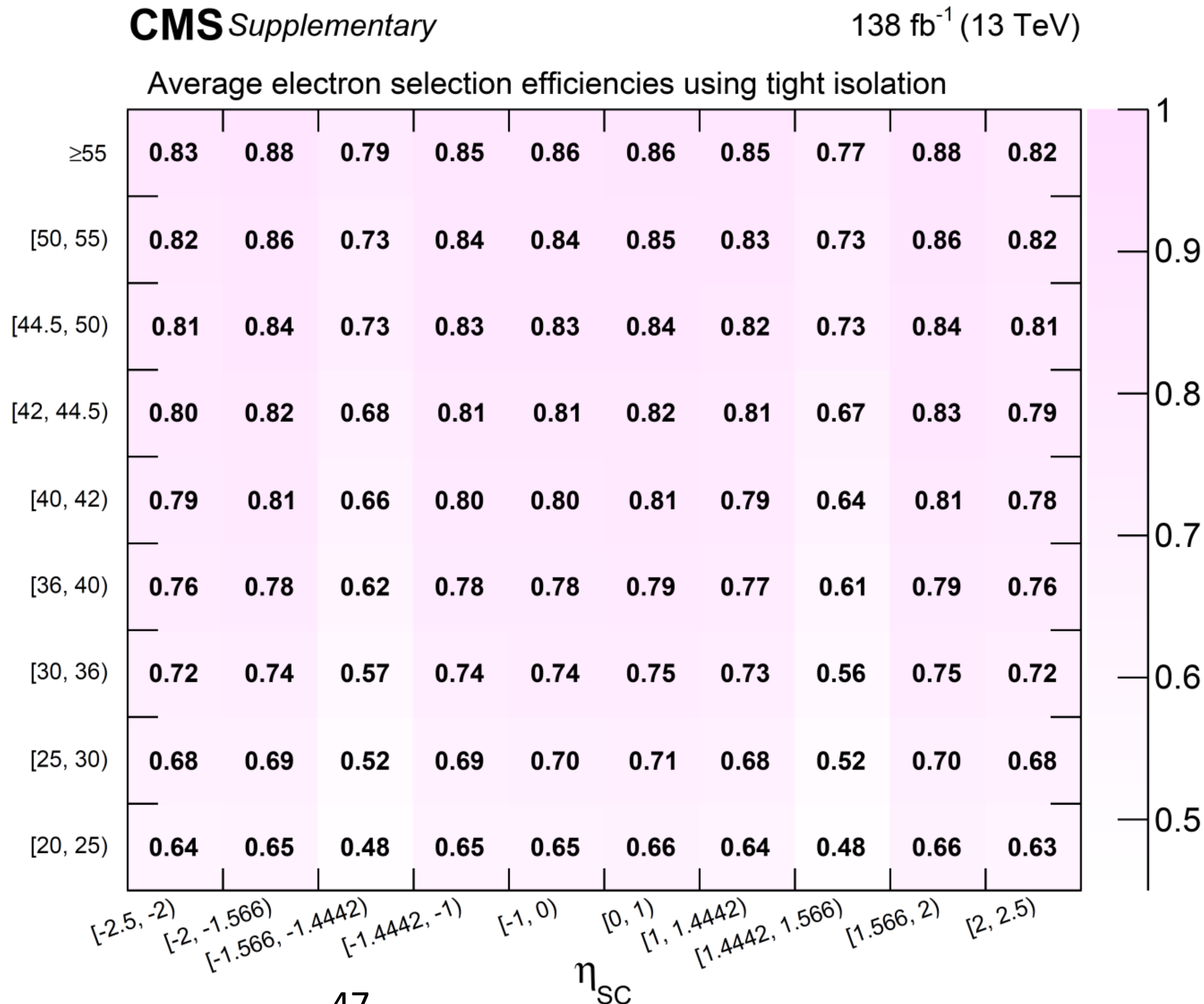

Transverse momentum of neutrinos

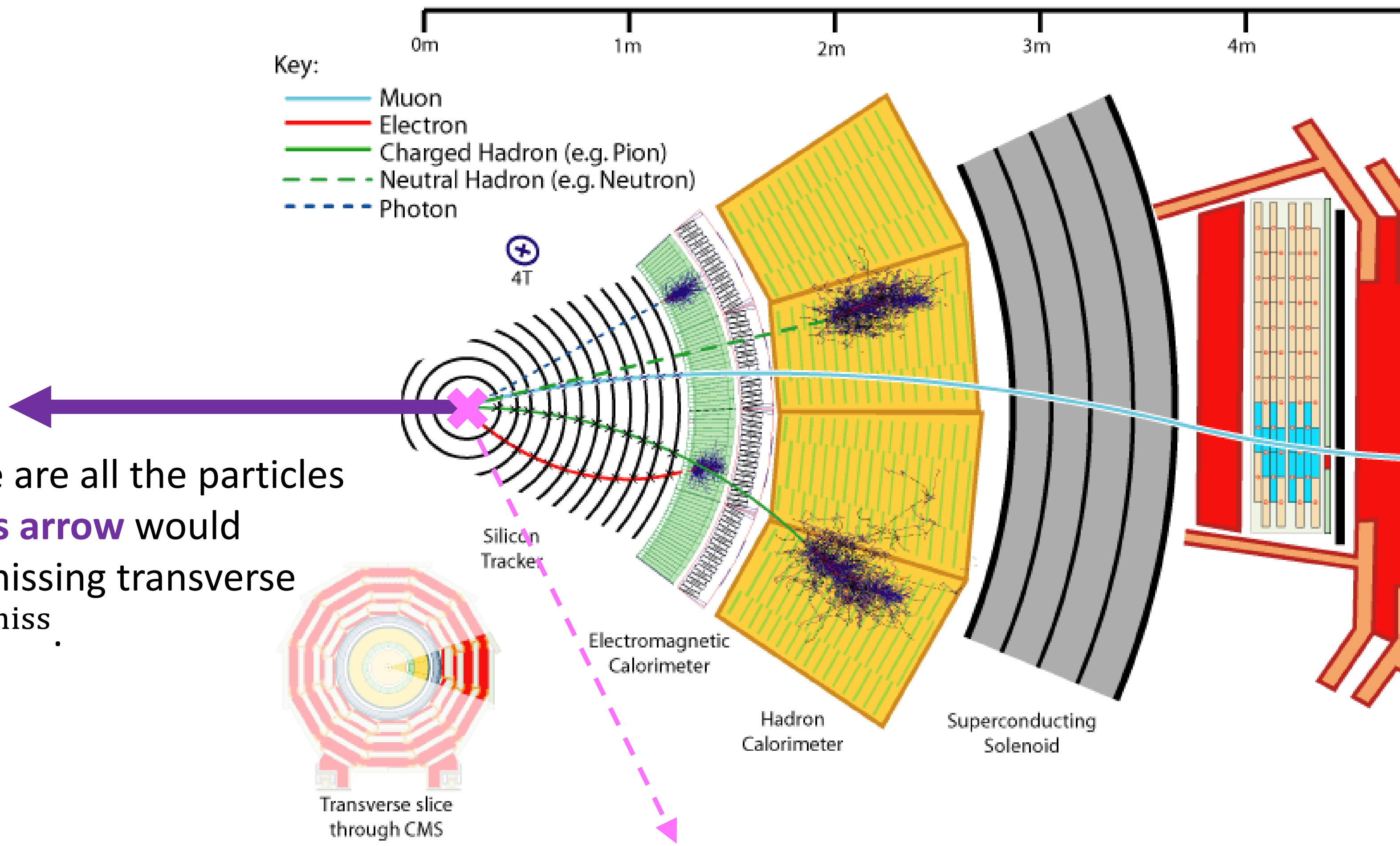

Assuming these are all the particles in an event, **this arrow** would represent the missing transverse momentum, $p_{\mathrm{T}}^{\mathrm{miss}}$.

Total transverse momentum from the collision should be 0.

Off-shell & BSM ggH couplings

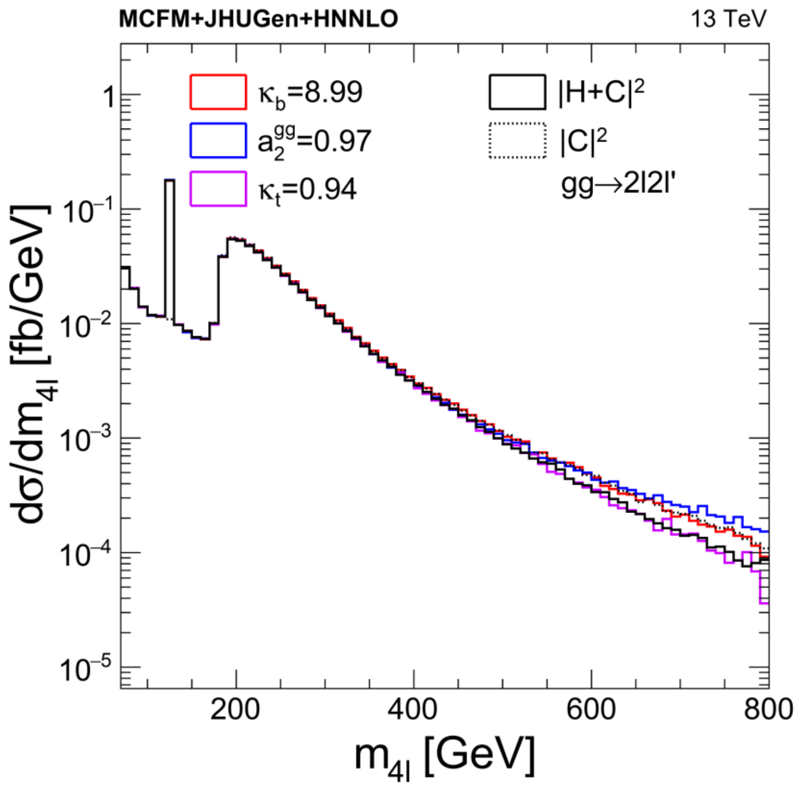

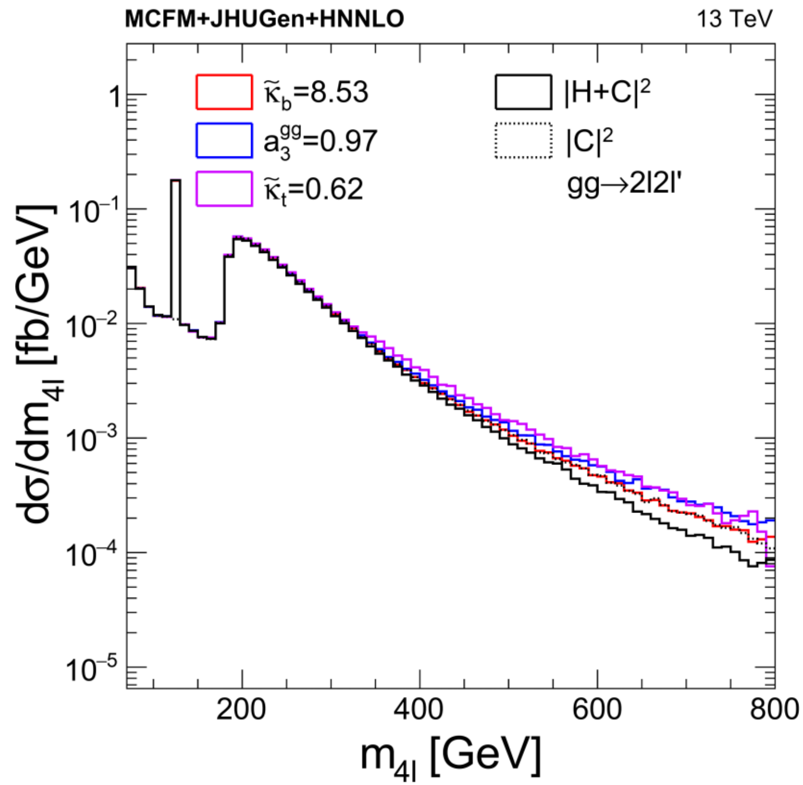

$$A(ggH) \sim \sum_f \kappa_f F_f(q_1, q_2|m_f) + \tilde{\kappa}_f \tilde{F}_f(q_1, q_2|m_f)$$
$$+ |a_2|\, e^{i\phi_{a2}}\, f^{*(1)}_{\mu\nu} f^{*(2),\mu\nu} + |a_3|\, e^{i\phi_{a3}}\, f^{*(1)}_{\mu\nu} \tilde{f}^{*(2),\mu\nu}$$

Effects [1] only visible for a *purely BSM Higgs boson* beyond ~500 GeV, couplings constrained to a fraction of these values [2]

Similar conclusions from couplings that affect the continuum [3,4]

No sensitivity with current number of events, so we assume gg couplings are as in the SM.

[1] Sarica, U. Springer Theses (2019)
[2] CMS Collaboration; arxiv:2205.05120 (2022)
[2] LHC Higgs Off-shell Subgroup; CDS:2801789 (2022)
[3] SMEFiT Collaboration; JHEP 11 089 (2021)

Gluon fusion: Higgs amplitude

$gg \to H \to ZZ$:

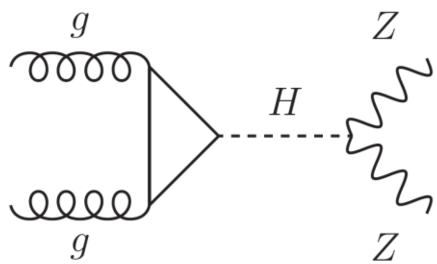

Full cross section calculation is available at different orders for the different components:
→ $gg \to H \to ZZ$: $\mathrm{N^3LO}$ in QCD around $m_H = 125$ GeV, NNLO for the full m_{ZZ} dependence, NLO or LO for event simulation [1]
→ K-factors are large for NLO/LO (~1.7-1.8), smaller and flatter for NNLO/NLO (~1.2-1.3), and the $\mathrm{N^3LO}$/NNLO K-factor is 1.10.

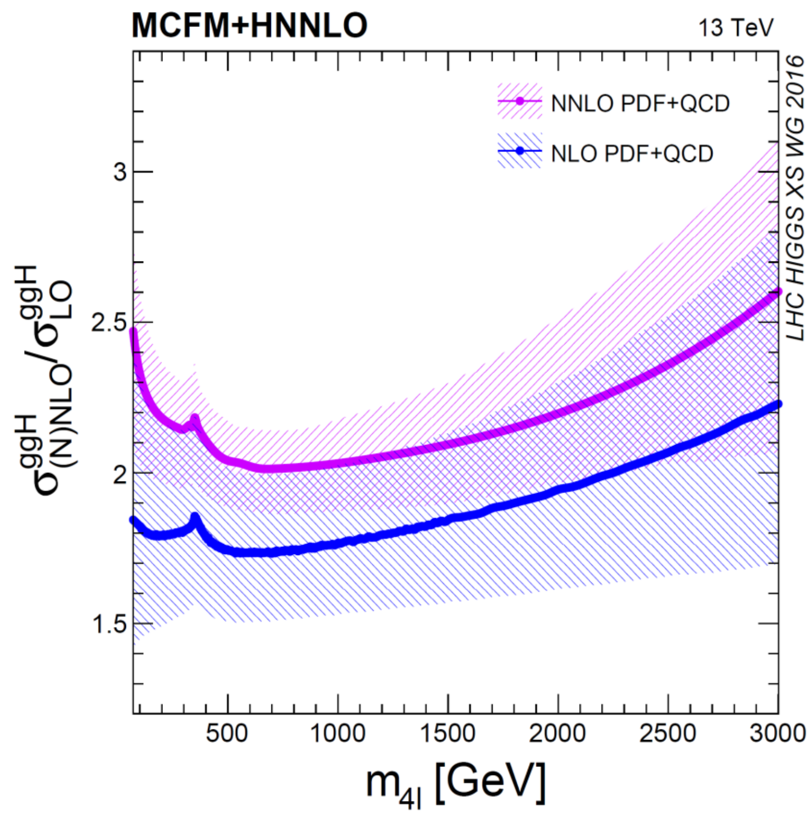

[1] LHC Higgs WG; CERN-2017-002-M

Gluon fusion: Continuum amplitude

$gg \to ZZ$:

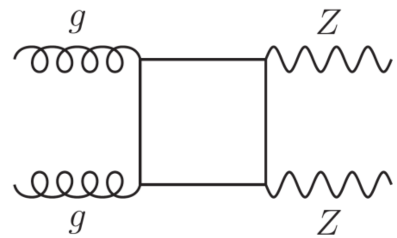

Full cross section calculation is available at different orders for the different components:
→ $gg \to ZZ$ continuum (and interference): Only full calculation and simulation with loop effects available at LO in QCD

- → Approximate NLO calculations [1] show K-factors for $gg \to ZZ$ continuum, $gg \to H \to ZZ$, and their interference within ~10% suggesting corrections are mostly of soft/collinear nature
- → CMS procedure is to use K-factors for $gg \to H \to ZZ$ on all components, and unc. $\kappa_{ggZZ} = 1 \pm 0.1$ on continuum with related scale $\sqrt{\kappa_{ggZZ}}$ on interference.

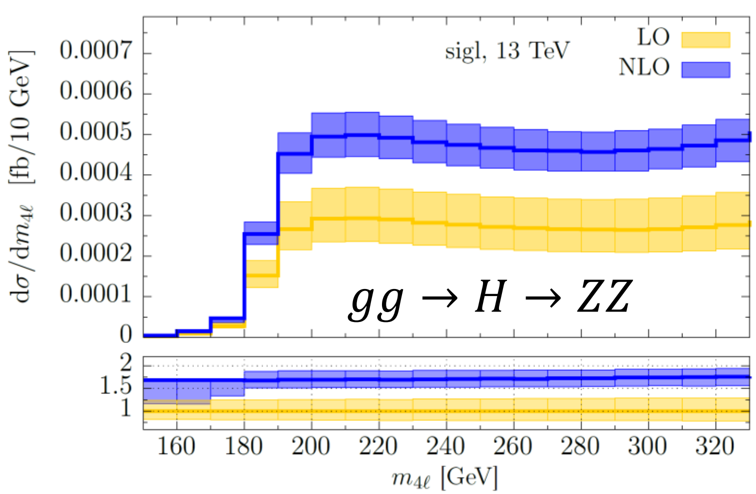

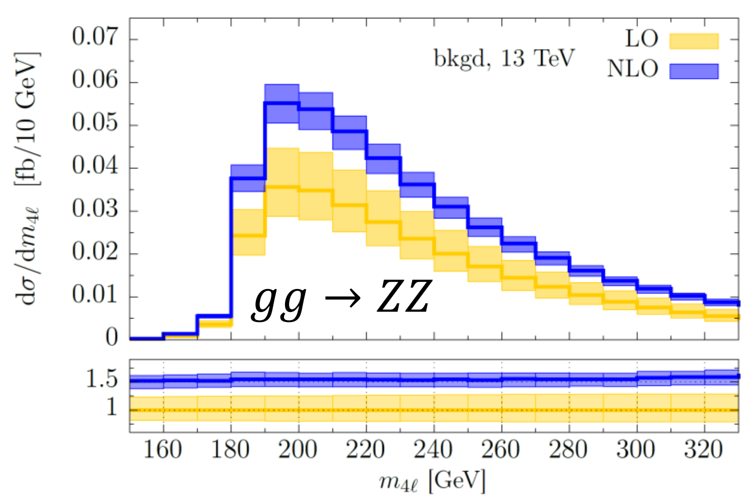

[1] Caola, F. et al.; JHEP 07 087 (2016)

Gluon fusion: Continuum amplitude

$gg \to ZZ$:

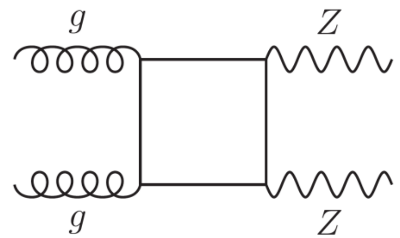

Full cross section calculation is available at different orders for the different components:

→ $gg \to ZZ$ continuum (and interference): Only full calculation and simulation with loop effects available at LO in QCD

- → Approximate NLO calculations [1] show K-factors for $gg \to ZZ$ continuum, $gg \to H \to ZZ$, and their interference within ~10% suggesting corrections are mostly of soft/collinear nature
- → ATLAS procedure is to use separate NLO mass-dependent K-factors with x1.2 for NNLO and x1.1 for N3LO scaling in QCD.

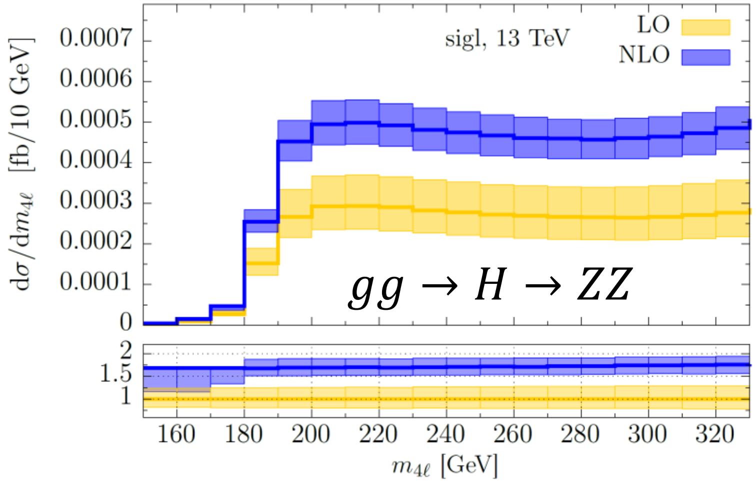

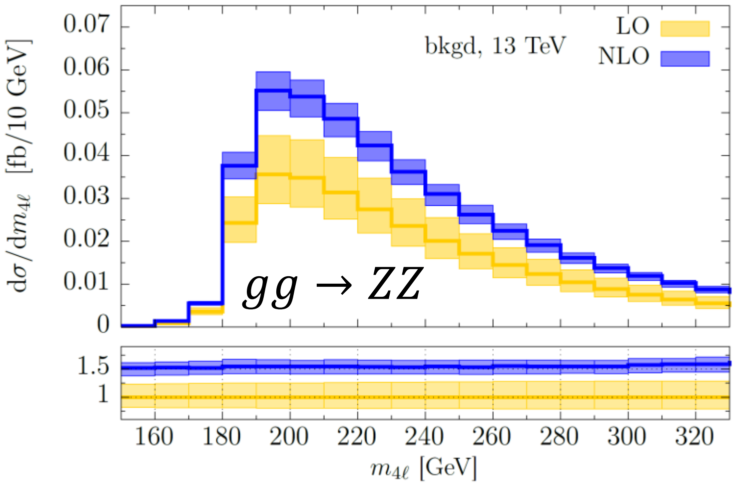

[1] Caola, F. et al.; JHEP 07 087 (2016)

Gluon fusion: Continuum amplitude

$gg \to ZZ$:

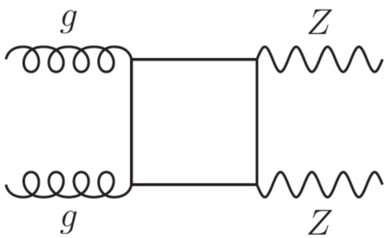

Full cross section calculation is available at different orders for the different components:
→ $gg \to ZZ$ continuum (and interference): Only full calculation and simulation with loop effects available at LO in QCD

- → Approximate NLO calculations [1] show K-factors for $gg \to ZZ$ continuum, $gg \to H \to ZZ$, and their interference within ~10% suggesting corrections are mostly of soft/collinear nature
- → ATLAS unc. doubled for $p_{\mathrm{T}}^{ZZ} > 150$ GeV; +50% when $m_{ZZ} \sim 2m_t$

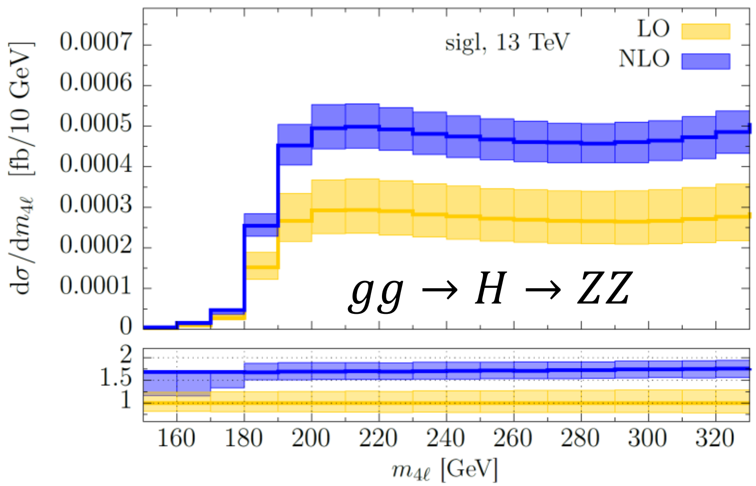

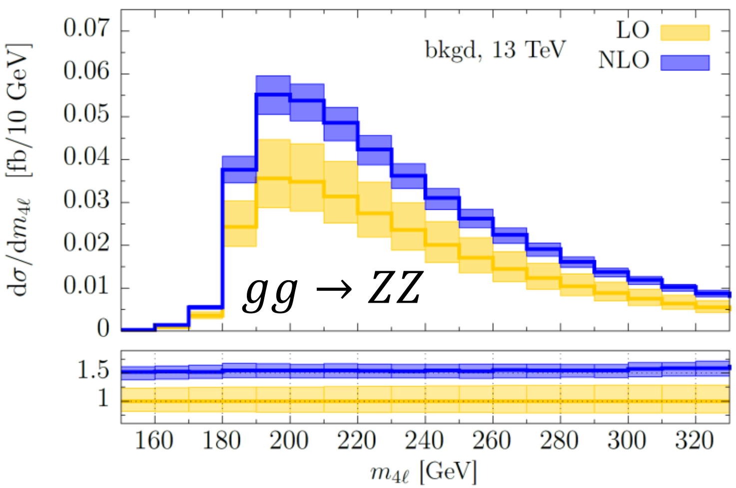

[1] Caola, F. et al.; JHEP 07 087 (2016)

Gluon fusion: Event generation in CMS

For the Higgs amplitude contribution, continuum ZZ, or interference, MC event generation can be done in two ways [1]:

→ Use JHUGen/MCFM to produce events at LO in QCD, apply NNLO K-factors and $\mathrm{N^3LO}$ flat normalization

→ Relies on Pythia for jet multiplicity and kinematics

→ Use POWHEG to produce $gg \to H$, JHUGen for $H \to ZZ$, and the MELA matrix elements from JHUGen/MCFM (instead of event generation) to obtain continuum ZZ and interference.

→ POWHEG cannot produce off-shell line shape. Instead, produce samples for Higgs samples at m_H =125, 160 ... 200 ... 3000 GeV, which have increasingly larger widths.

→ $\mathrm{hfact} = m_H/10 + 37.5$ GeV to match p_T^H to NNLO+NNLL HRES predictions.

→ For the $gg \to H(125) \to ZZ$ amplitude, the only differences in these samples are the propagator and the correction of the m_{ZZ} line shape for the evolution of BR($H \to ZZ$).

The former is just reweighting the propagator to a BW($m_H = 125$ GeV, $\Gamma_H = 4.1$ MeV), so it is basically part of the MELA reweighting procedure, and the latter is added as a modification of event weights when running the JHUGen decay step.

→ The samples are glued together in the end to produce the full spectrum. The mathematical formulation is provided extensively in the note.

→ We observe this approach produces stable results in jet multiplicity and other kinematics after Pythia parton shower.

[1] CMS Collaboration; CMS-NOTE-2022-010, CDS:2826782

Gluon fusion: Jet-exclusive comparisons

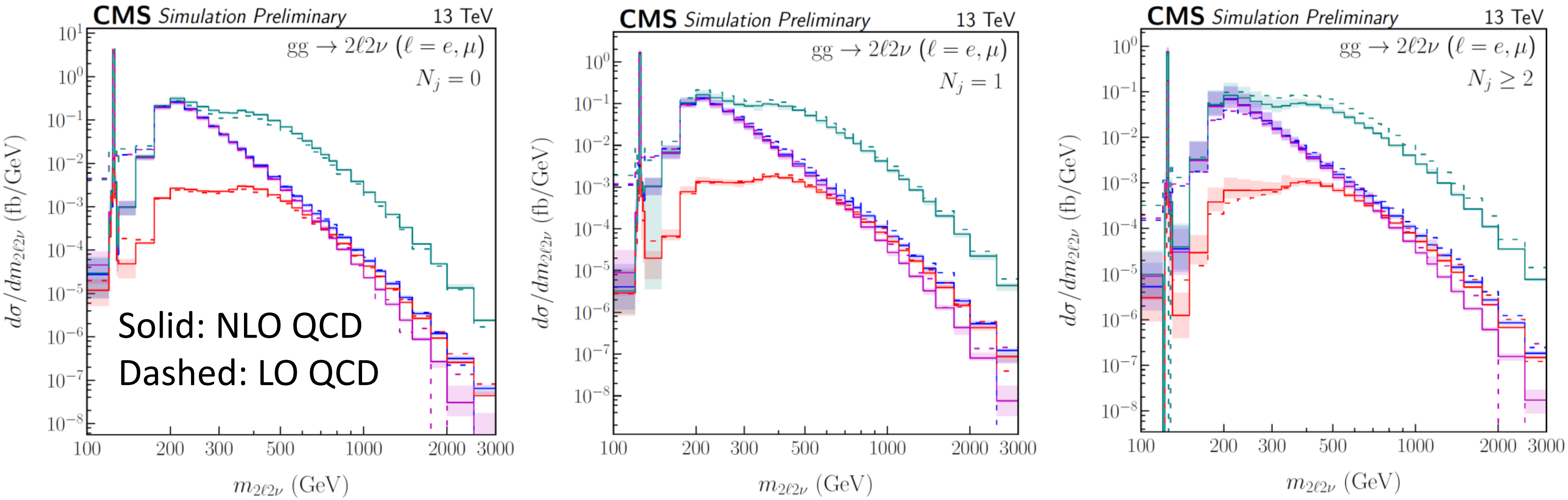

Analyses need better control over jet multiplicity and kinematics than what MC LO in QCD + parton shower can provide.

When split by jet (*) multiplicity, $N_j = 0{,}1$ have similar levels of agreement
→ LO m_{ZZ} distortion at $N_j \geq 2$ understood to be because of parton shower effects

(*) Gen.-level anti-k$_\mathrm{T}$ $\Delta R = 0.4$ jets with $p_T > 30$ GeV, $|\eta| < 4.7$

[1] CMS Collaboration; CMS-NOTE-2022-010, CDS:2826782

EW production simulation in CMS

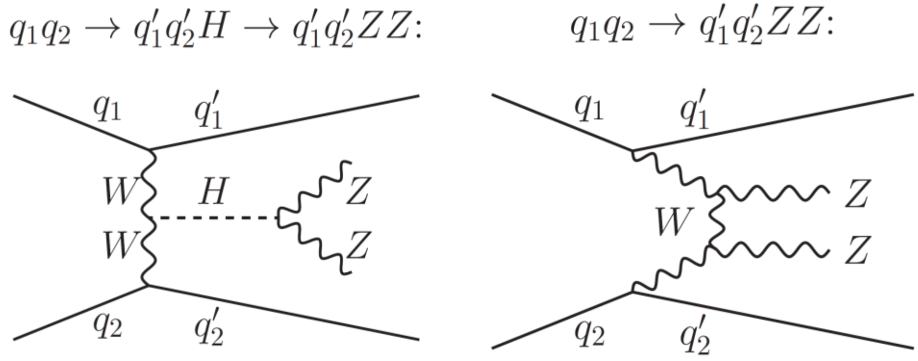

Matrix element (MELA) and event simulation (MCFM/JHUGen) available for SM or BSM Higgs hypotheses, and continuum at LO in QCD consistently.

→ Improve event simulation technique for jet kinematics [1] by

- starting with POWHEG+JHUGen samples for NLO VBF, and ZH and WH NLO + MiNLO HVJ)
- apply MELA ME reweighting

→ Account for the extra partons from POWHEG by merging four-momenta of gluons (or $g \to q\bar{q}$ decays) to the closest quark

→ We check that the LO topology is approximated decently.

[1] CMS Collaboration; CMS-NOTE-2022-010, CDS:2826782

EW process: Jet-exclusive comparisons

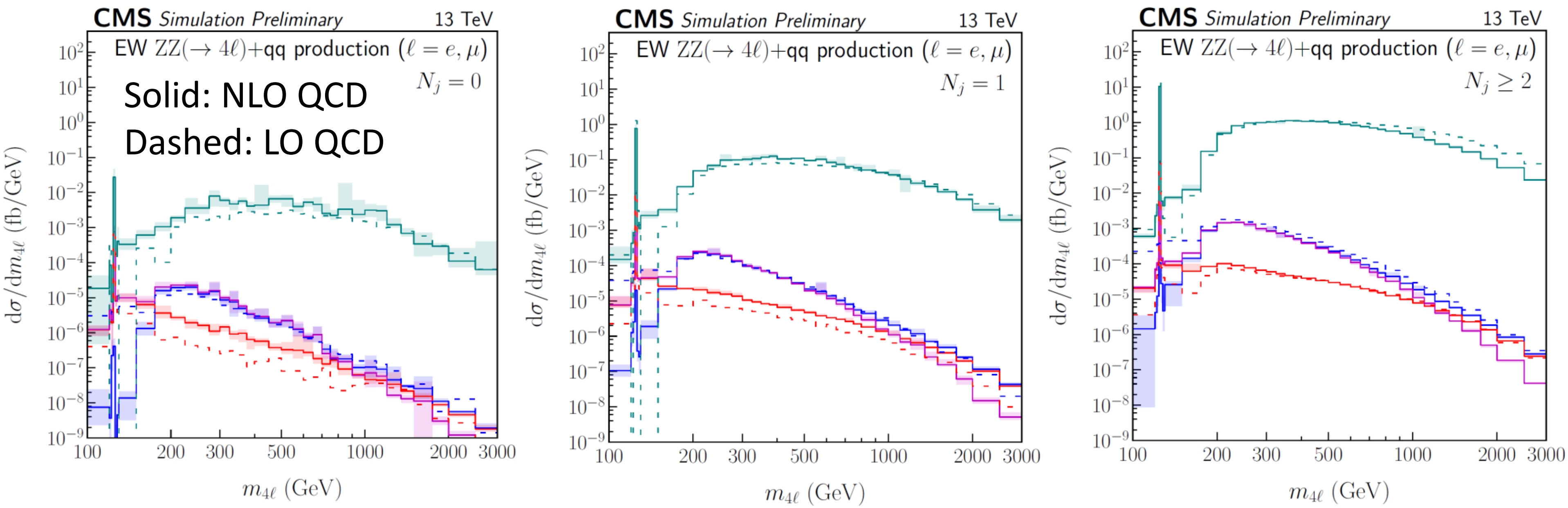

Analyses need better control over jet multiplicity and kinematics than what MC LO in QCD + parton shower can provide.

When events are split by jet multiplicity and equivalent selection requirements are placed on the LO and NLO MC, we find differences in $N_j = 0{,}1$.
→ Discrepancies are understood to be from imprecise parton shower modelling in the LO MC.

[1] CMS Collaboration; CMS-NOTE-2022-010, CDS:2826782

EW processes: Recasting NLO topology to LO

The MELA and MELAANALYTICS packages impose several rules on the merging procedure for the EW processes in order to make sensible predictions:

- An incoming gluon is never merged into an incoming quark. This rule is invoked implicitly as the q^2 of the incoming partons is always the largest compared to that of any other pair of partons in the event.
- Gluons are never merged into the decay products of the H boson from the JHUGen step as they are produced during the production of the H boson with no prior knowledge about the boson's decay.
- Gluons are also never merged into the decay products of the associated W or Z boson in the VH samples. Doing so distorts the BW nature of these resonances significantly.
- All merging is done in the convention of outgoing particles. This means the four-momenta and charge of incoming particles are reversed in the intermediate steps when those of the two merged particles are summed.
- When an incoming gluon is merged into an outgoing quark, the charge (i.e., PDG id) and the four-momentum of the quark are reversed in the final step of the LO topology construction. This reversion is done so that the event topology ensures having exactly two incoming quarks as expected in the LO matrix elements.
- In the VH samples, when extra gluons are encountered, the merging of individual gluons and that of a combined gluon (i.e., from a $g \to gg$ process) are all considered separately.
- In the VH samples, it is also possible to encounter two extra quarks instead of gluons. These extra quarks are merged into a gluon substitute first, as they are from a $g \to q\bar{q}$ branching process, before the merging of this gluon substitute is considered.
- Every merging permutation is considered, rated with the product of the dot-products between the merged quarks and gluons, and those that do not produce an incoming-outgoing parton composition that is compatible with the main physics process of the sample (i.e., VBF, ZH, or WH) are skipped.
- A momentum redistribution procedure is applied on the incoming and outgoing particles associated with H boson production so that the resultant topology features massless particles, which is what is required from the use of massless spinors in matrix elements. Denoting the momenta of the two final incoming or outgoing partons as p_1 and p_2, an intermediate four-momentum k is added to p_1 and subtracted from p_2 such that $|p_1 + k|^2 = |p_2 - k|^2 = 0$. This step is common to any matrix element computed using the MELA package. Because event-by-event reweighting is done through a ratio of matrix elements, which are invariant under any arbitrary boost of the event topology, and because factors coming from PDFs cancel in the ratio, the common boost of all particles does not affect reweighting as long as momentum conservation is maintained strictly, and is therefore adjusted arbitrarily.

[1] CMS Collaboration; CMS-NOTE-2022-010, CDS:2826782

$q\bar{q} \to ZZ, WZ$ simulation (CMS)

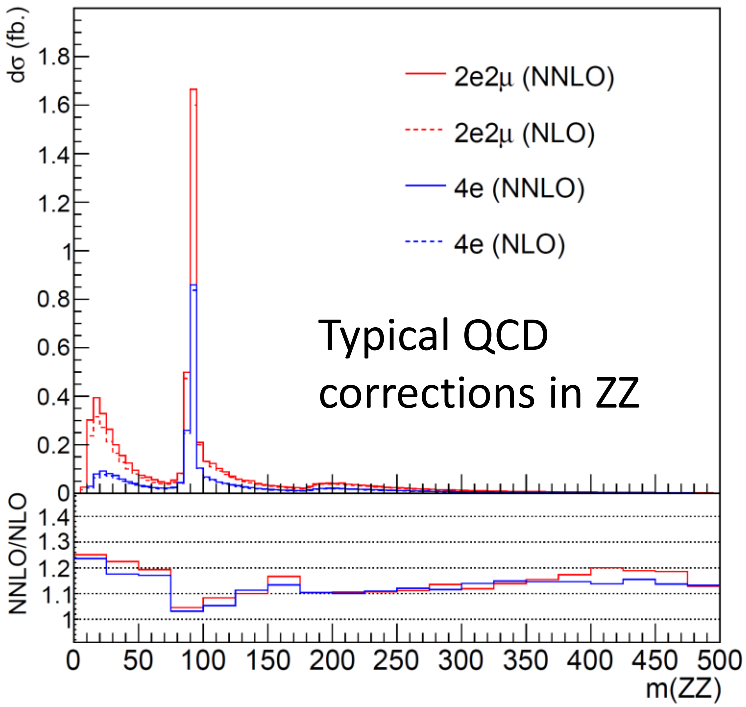

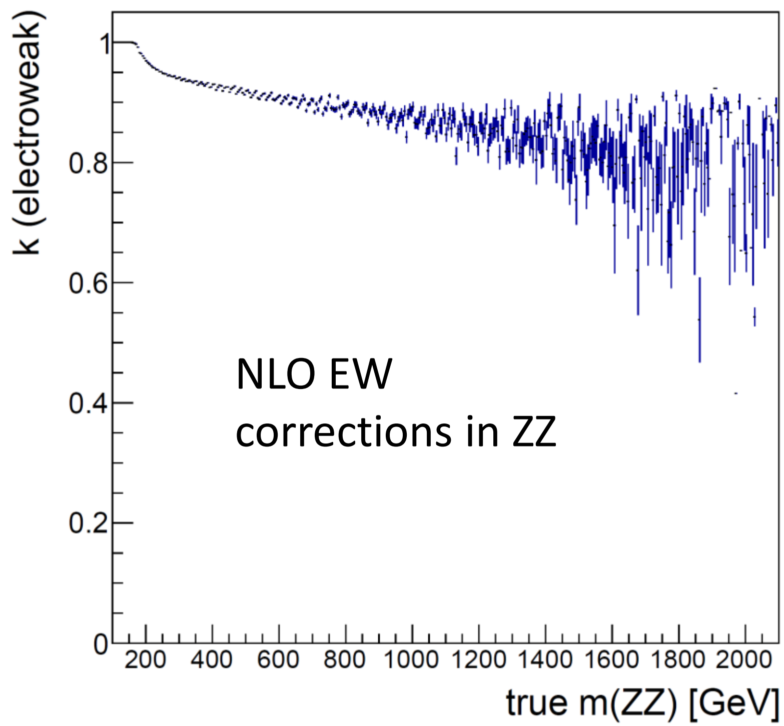

POWHEG simulation at NLO in QCD in CMS for the non-interfering ZZ and WZ backgrounds.
→ NNLO QCD corrections calculated as a function of m_{ZZ}
→ Relative uncertainties from the MC close to NNLO QCD cross section uncertainties
→ Keep the relative uncs. as in the MC to predict the uncertainty in different kinematic regions and jet categories

$q\bar{q} \rightarrow ZZ, WZ$ simulation (CMS)

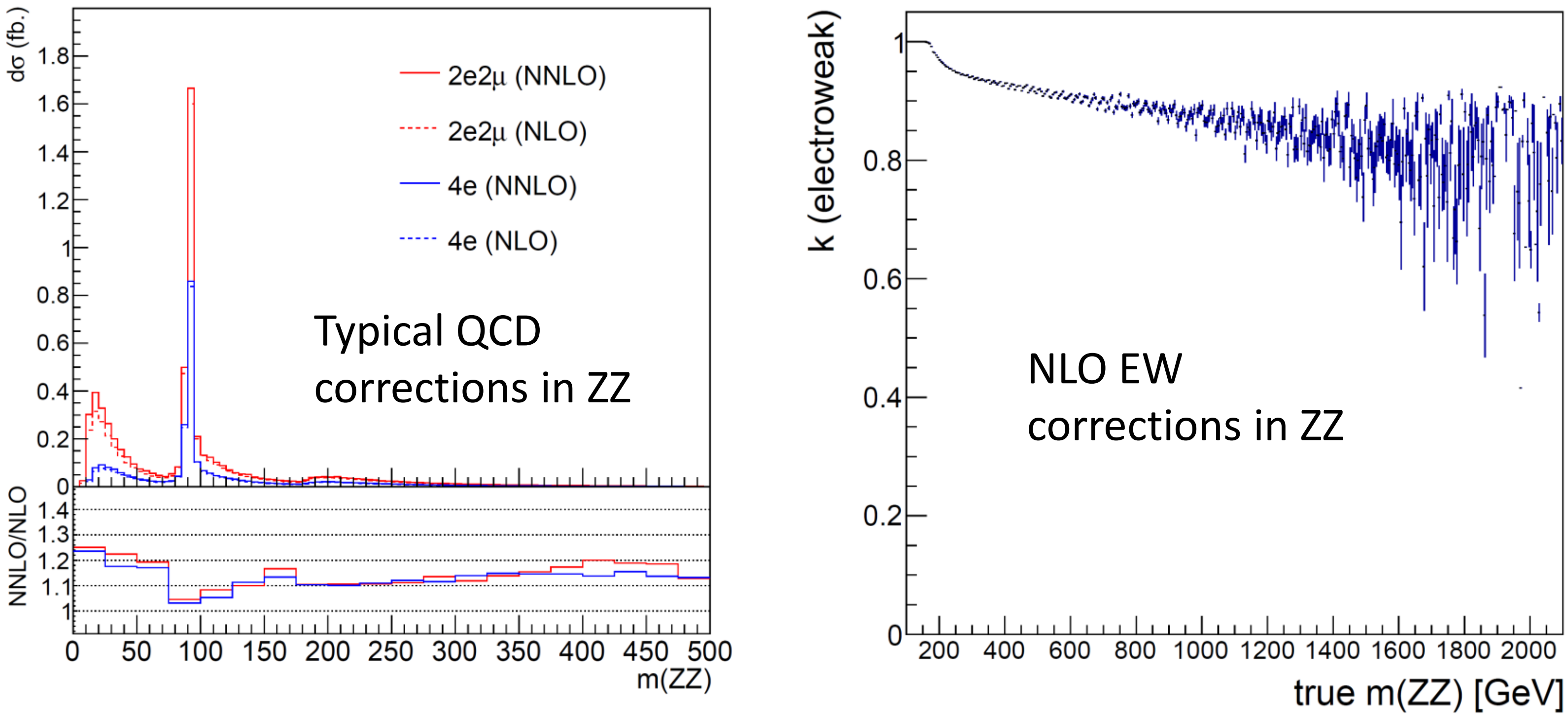

POWHEG simulation at NLO in QCD in CMS for the non-interfering ZZ and WZ backgrounds.
→ NLO EW corrections typically reach -20% in ZZ (-10% in WZ) at ~1 TeV [1].

→ Assign the following uncertainty prescription [2] based on $\rho = \frac{\left|\sum_i \vec{p}_T^{\,i}\right|}{\sum_i \left|\vec{p}_T^{\,i}\right|}$ over leptons:

$$\delta = \begin{cases} \left(1 - K_{QCD}^{NLO}\right)\left(1 - K_{EW}^{NLO}\right) \text{ if } \rho < 0.3 \\ \left(1 - K_{EW}^{NLO}\right) \qquad \text{otherwise} \end{cases}$$

[1] Bierweiler, A. et al.; JHEP 12 071 (2013)
[2] Gieseke, S. et al.; EPJ C 74 2988 (2014)

$q\bar{q} \rightarrow ZZ, WZ$ simulation (ATLAS)

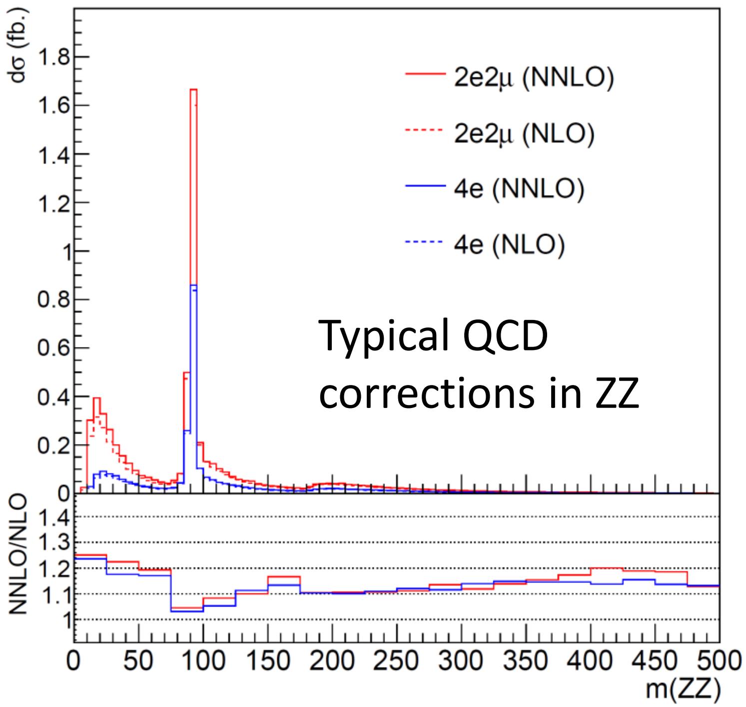

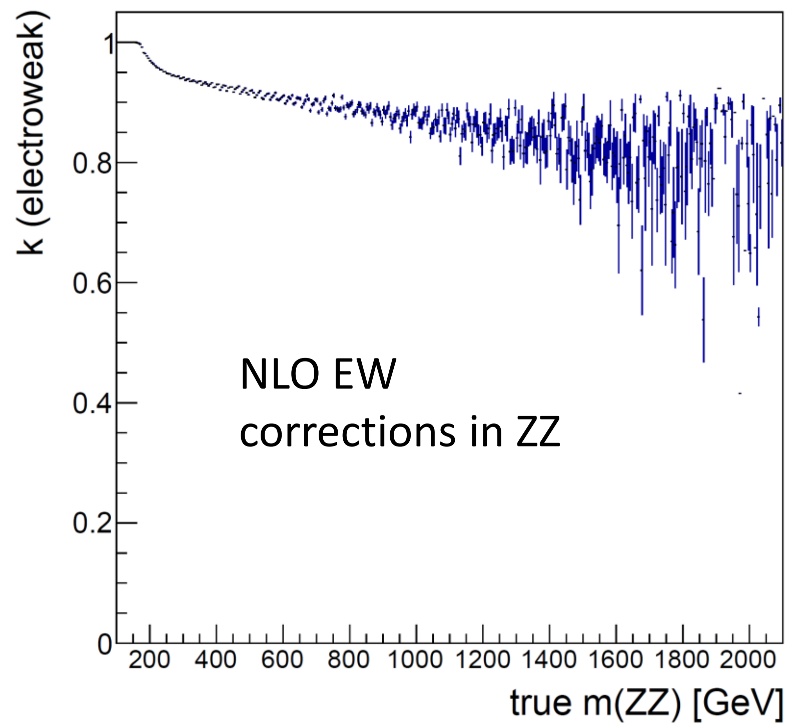

ATLAS uses Sherpa @NLO (LO) in 0+1 jet (2+3 jets)
→ Uncertainties independent in N_j categories
→ Overall normalizations obtained from CRs
→ For NLO EW corrections, 4ℓ assigns corr. over m_{ZZ} w/ uncs. as in [1]
→ $2\ell2\nu$ averages multiplicative and additive NLO QCD(+)EW corrections, assigns difference as unc.

[1] Gieseke, S. et al.; EPJ C 74 2988 (2014)

CMS analysis ingredients

Need high-mass ZZ events that contain off-shell Higgs boson contributions
→ Can be done in both 4ℓ (high-m_{4l}) and $2\ell 2\nu$ (high-m_{T}^{ZZ}) final states
→ $\mathrm{BR}(2\ell 2\nu) \sim 6 \times \mathrm{BR}(4\ell)$
→ 4ℓ cleaner in bkgs. (only irreducible) while $2\ell 2\nu$ also has instrumental components.
→ About equal statistical importance in the results from the two channels

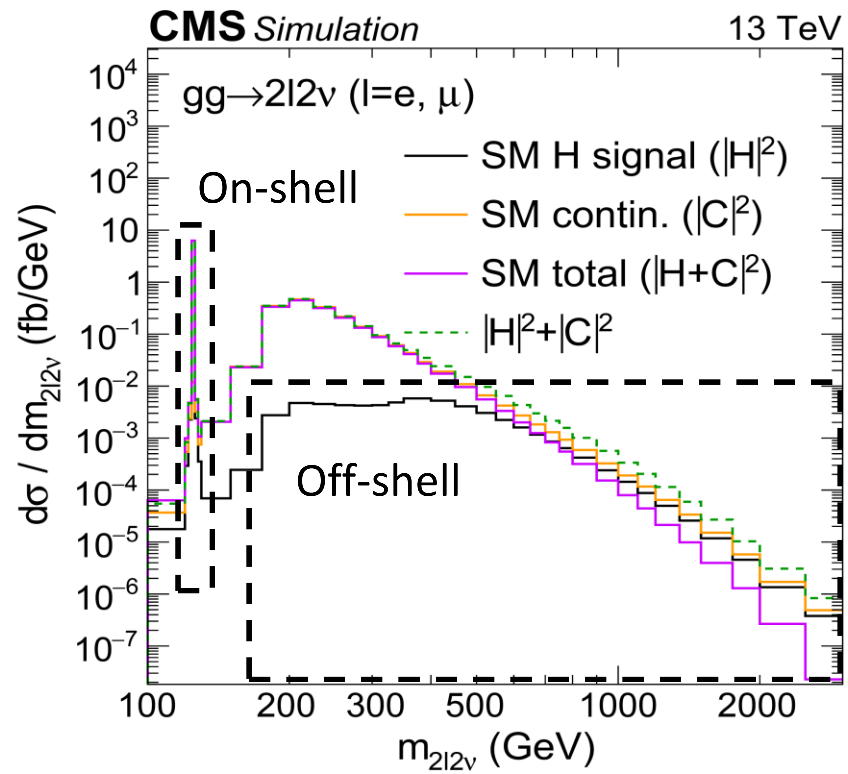

Need on-shell $\mathrm{H}(125)$ events to extract Γ_{H}
→ 4ℓ only (not possible with neutrinos)
→ Little background

Extract physics using a combined fit to 117 multidimensional distributions:
24 distributions in off-shell $2\ell 2\nu$ (2326 events)
→ Analysis also combines 18 distributions from a $WZ \to 3\ell\nu$ CR (8541 events)
18 distributions in off-shell 4ℓ (1407 events), and 57 distributions in on-shell 4ℓ (621 events)

In off-shell categories, event counts are typically different from the SM by ~10-50% (larger at higher masses) for $\mu^{\mathrm{off-shell}} = 0$ (or ~2.5)

CMS analysis ingredients

Need high-mass ZZ events that contain off-shell Higgs boson contributions

→ Can be done in both 4ℓ (high-m_{4l}) and $2\ell 2\nu$ (high-m_{T}^{ZZ}) final states

→ $\mathrm{BR}(2\ell 2\nu) \sim 6 \times \mathrm{BR}(4\ell)$

→ 4ℓ cleaner in bkgs. (only irreducible) while $2\ell 2\nu$ also has instrumental components.

→ About equal statistical importance in the results from the two channels

Need on-shell $\mathrm{H}(125)$ events to extract Γ_{H}

→ 4ℓ only (not possible with neutrinos)

→ Little background

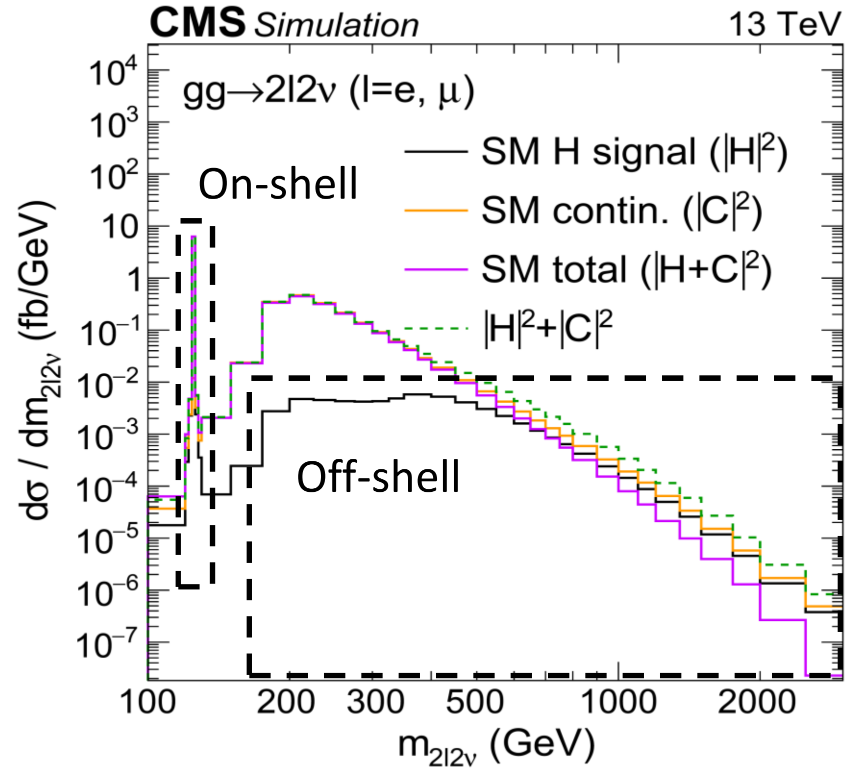

Biggest challenge in analysis is to extract off-shell information from the tails:

→ Limited statistics, e.g., in $2\ell 2\nu$ with $N_j \geq 2$, $p_{\mathrm{T}}^{\mathrm{miss}} > 200$ GeV, and $m_{\mathrm{T}}^{ZZ} > 450$ GeV, off-shell $|\mathrm{H}|^2$:H-C interf.:total expected = 10:-17:64 (events)

→ Need precise control over instrumental and irreducible backgrounds

→ Need theory input, e.g. for NLO EW corrections in $q\bar{q} \to ZZ, WZ$, for increased precision

Full table of observables for CMS off-shell 4ℓ

Category	VBF-tagged	VH-tagged	Untagged
Selection	$\mathcal{D}_{\text{2jet}}^{\text{VBF}}$ or $\mathcal{D}_{\text{2jet}}^{\text{VBF,BSM}} > 0.5$	$\mathcal{D}_{\text{2jet}}^{\text{WH}}$ or $\mathcal{D}_{\text{2jet}}^{\text{WH,BSM}}$, or $\mathcal{D}_{\text{2jet}}^{\text{ZH}}$ or $\mathcal{D}_{\text{2jet}}^{\text{ZH,BSM}} > 0.5$	Rest of events
SM obs.	$m_{4\ell}, \mathcal{D}_{\text{bkg}}^{\text{VBF+dec}}, \mathcal{D}_{\text{bsi}}^{\text{VBF+dec}}$	$m_{4\ell}, \mathcal{D}_{\text{bkg}}^{\text{VH+dec}}, \mathcal{D}_{\text{bsi}}^{\text{VH+dec}}$	$m_{4\ell}, \mathcal{D}_{\text{bkg}}^{\text{kin}}, \mathcal{D}_{\text{bsi}}^{\text{gg,dec}}$
a_3 obs.	$m_{4\ell}, \mathcal{D}_{\text{bkg}}^{\text{VBF+dec}}, \mathcal{D}_{0-}^{\text{VBF+dec}}$	$m_{4\ell}, \mathcal{D}_{\text{bkg}}^{\text{VH+dec}}, \mathcal{D}_{0-}^{\text{VH+dec}}$	$m_{4\ell}, \mathcal{D}_{\text{bkg}}^{\text{kin}}, \mathcal{D}_{0-}^{\text{dec}}$
a_2 obs.	$m_{4\ell}, \mathcal{D}_{\text{bkg}}^{\text{VBF+dec}}, \mathcal{D}_{0h+}^{\text{VBF+dec}}$	$m_{4\ell}, \mathcal{D}_{\text{bkg}}^{\text{VH+dec}}, \mathcal{D}_{0h+}^{\text{VH+dec}}$	$m_{4\ell}, \mathcal{D}_{\text{bkg}}^{\text{kin}}, \mathcal{D}_{0h+}^{\text{dec}}$
Λ_1 obs.	$m_{4\ell}, \mathcal{D}_{\text{bkg}}^{\text{VBF+dec}}, \mathcal{D}_{\Lambda 1}^{\text{VBF+dec}}$	$m_{4\ell}, \mathcal{D}_{\text{bkg}}^{\text{VH+dec}}, \mathcal{D}_{\Lambda 1}^{\text{VH+dec}}$	$m_{4\ell}, \mathcal{D}_{\text{bkg}}^{\text{kin}}, \mathcal{D}_{\Lambda 1}^{\text{dec}}$

Full table of observables for CMS on-shell 4ℓ

2016-2018 categorization follows the order
- VBF-2 jet
- VH-hadronic
- VH-leptonic (1 lepton or an $\ell^+\ell^-$ pair)
- VBF-1 jet
- Boosted
- Untagged

Category	Selection	Observables $\vec{x}$ for fitting
Boosted	$p_{\mathrm{T}}^{4\ell} > 120\,\mathrm{GeV}$	$\mathcal{D}_{\mathrm{bkg}}, p_{\mathrm{T}}^{4\ell}$
VBF-1jet	$\mathcal{D}_{\mathrm{1jet}}^{\mathrm{VBF}} > 0.7$	$\mathcal{D}_{\mathrm{bkg}}, p_{\mathrm{T}}^{4\ell}$
VBF-2jet	$\mathcal{D}_{\mathrm{2jet}}^{\mathrm{VBF}} > 0.5$	$\mathcal{D}_{\mathrm{bkg}}^{\mathrm{EW}}, \mathcal{D}_{0h+}^{\mathrm{VBF+dec}}, \mathcal{D}_{0-}^{\mathrm{VBF+dec}}, \mathcal{D}_{\Lambda 1}^{\mathrm{VBF+dec}}, \mathcal{D}_{\Lambda 1}^{Z\gamma,\mathrm{VBF+dec}}, \mathcal{D}_{\mathrm{int}}^{\mathrm{VBF}}, \mathcal{D}_{CP}^{\mathrm{VBF}}$
VH-hadronic	$\mathcal{D}_{\mathrm{2jet}}^{\mathrm{VH}} > 0.5$	$\mathcal{D}_{\mathrm{bkg}}^{\mathrm{EW}}, \mathcal{D}_{0h+}^{\mathrm{VH+dec}}, \mathcal{D}_{0-}^{\mathrm{VH+dec}}, \mathcal{D}_{\Lambda 1}^{\mathrm{VH+dec}}, \mathcal{D}_{\Lambda 1}^{Z\gamma,\mathrm{VH+dec}}, \mathcal{D}_{\mathrm{int}}^{\mathrm{VH}}, \mathcal{D}_{CP}^{\mathrm{VH}}$
VH-leptonic	see Section 3	$\mathcal{D}_{\mathrm{bkg}}, p_{\mathrm{T}}^{4\ell}$
Untagged	none of the above	$\mathcal{D}_{\mathrm{bkg}}, \mathcal{D}_{0h+}^{\mathrm{dec}}, \mathcal{D}_{0-}^{\mathrm{dec}}, \mathcal{D}_{\Lambda 1}^{\mathrm{dec}}, \mathcal{D}_{\Lambda 1}^{Z\gamma,\mathrm{dec}}, \mathcal{D}_{\mathrm{int}}^{\mathrm{dec}}, \mathcal{D}_{CP}^{\mathrm{dec}}$

Off-shell $2\ell 2\nu$: CMS event selection

Quantity	Requirement
p_T^ℓ	$p_T^\ell \geq 25\,\mathrm{GeV}$ on both leptons
$\lvert\eta_\ell\rvert$	< 2.4 on μ, < 2.5 on e
$m_{\ell\ell}$	$\lvert m_{\ell\ell} - 91.2\rvert < 15\,\mathrm{GeV}$
$p_T^{\ell\ell}$	$\geq 55\,\mathrm{GeV}$
N_ℓ	Exactly two leptons with tight isolation, no extra leptons with loose isolation and $p_T \geq 5\,\mathrm{GeV}$
N_{trk}	No isolated tracks satisfying the selection requirements
N_γ	No photons with $p_T \geq 20\,\mathrm{GeV}$, $\lvert\eta\rvert < 2.5$ satisfying the baseline selection requirements
p_T^j	$\geq 30\,\mathrm{GeV}$, used in selecting jets
$\lvert\eta_j\rvert$	< 4.7, used in selecting jets
N_b	No b-tagged jets based on the loose working point
p_T^{miss}	$\geq 125\,\mathrm{GeV}$ if $N_j < 2$, $\geq 140\,\mathrm{GeV}$ otherwise
$\Delta\phi_{miss}^{\ell\ell}$	> 1.0 between $\vec{p}_T^{\,\ell\ell}$ and $\vec{p}_T^{\,miss}$
$\Delta\phi_{miss}^{\ell\ell+jets}$	> 2.5 between $\vec{p}_T^{\,\ell\ell} + \sum \vec{p}_T^{\,j}$ and $\vec{p}_T^{\,miss}$
$\min \Delta\phi_{miss}^{j}$	> 0.25 if $N_j = 1$, > 0.5 otherwise among all $\vec{p}_T^{\,j}$ and $\vec{p}_T^{\,miss}$ combinations

Requirements are mainly aimed toward reducing
- instrumental p_T^{miss} smearing from Z+jets
- $t\bar{t} \rightarrow 2\ell 2\nu 2b$
- WW $\rightarrow 2\ell 2\nu$

Off-shell $2\ell 2\nu$: CMS $q\bar{q} \to ZZ, WZ$ CR

Quantity	Requirement
$p_{\mathrm{T}}^{\ell_{Z1}}$	$\geq 30\,\mathrm{GeV}$ on leading-p_{T} lepton forming the Z candidate
$p_{\mathrm{T}}^{\ell_{Z2}}$	$\geq 20\,\mathrm{GeV}$ on subleading-p_{T} lepton forming the Z candidate
$p_{\mathrm{T}}^{\ell_{W}}$	$\geq 20\,\mathrm{GeV}$ on the remaining ℓ_{W} from the W boson
$\lvert\eta_\ell\rvert$	< 2.4 on μ, < 2.5 on e
$m_{\ell\ell}$	Use the opposite-sign, same-flavor dilepton pair with smallest $\lvert m_{\ell\ell} - 91.2\rvert < 15\,\mathrm{GeV}$ to define the Z candidate
N_ℓ	Exactly three leptons with tight isolation, no extra leptons with loose isolation and $p_{\mathrm{T}} \geq 5\,\mathrm{GeV}$
N_{trk}	No isolated tracks satisfying the selection requirements
N_γ	No photons with $p_{\mathrm{T}} \geq 20\,\mathrm{GeV}$, $\lvert\eta\rvert < 2.5$ satisfying the baseline selection requirements
p_{T}^{j}	$\geq 30\,\mathrm{GeV}$, used in selecting jets
$\lvert\eta_j\rvert$	< 4.7, used in selecting jets
N_b	No b-tagged jets based on the loose working point
$p_{\mathrm{T}}^{\mathrm{miss}}$	$\geq 20\,\mathrm{GeV}$
$m_{\mathrm{T}}^{\ell_W}$	$\geq 20\,\mathrm{GeV}$ ($10\,\mathrm{GeV}$) for $\ell_W = \mu$ ($\ell_W = \mathrm{e}$), where $m_{\mathrm{T}}^{\ell_W} = \sqrt{2 p_{\mathrm{T}}^{\ell_W} p_{\mathrm{T}}^{\mathrm{miss}} \left(1 - \cos\Delta\phi_{\mathrm{miss}}^{\ell_W}\right)}$ is the transverse mass between $\vec{p}_{\mathrm{T}}^{\ell_W}$ and $\vec{p}_{\mathrm{T}}^{\mathrm{miss}}$
$\mathrm{A} \times m_{\mathrm{T}}^{\ell_W} + p_{\mathrm{T}}^{\mathrm{miss}} \geq 120\,\mathrm{GeV}$, with $\mathrm{A} = 1.6$ ($4/3$) for $\ell_W = \mu$ (e)	
$\Delta\phi_{\mathrm{miss}}^{\mathrm{Z}}$	> 1.0 between $\vec{p}_{\mathrm{T}}^{\mathrm{Z}}$ and $\vec{p}_{\mathrm{T}}^{\mathrm{miss}}$
$\Delta\phi_{\mathrm{miss}}^{3\ell+\mathrm{jets}}$	> 2.5 between $\vec{p}_{\mathrm{T}}^{3\ell} + \sum \vec{p}_{\mathrm{T}}^{\mathrm{j}}$ and $\vec{p}_{\mathrm{T}}^{\mathrm{miss}}$
$\min \Delta\phi_{\mathrm{miss}}^{\mathrm{j}}$	> 0.25 among all $\vec{p}_{\mathrm{T}}^{\mathrm{j}}$ and $\vec{p}_{\mathrm{T}}^{\mathrm{miss}}$ combinations

Estimated using POWHEG simulation at NLO in QCD
→ Additional K-factors for NLO EW and NNLO QCD corrections are applied.
→ A joint fit with a 3ℓ WZ CR is done with common nuisance parameters and m_{T}^{WZ} as the only observable:

$$m_{\mathrm{T}}^{\mathrm{WZ}^2} = \left[\sqrt{p_{\mathrm{T}}^{\ell\ell^2} + m_{\ell\ell}^2} + \sqrt{\left|\vec{p}_{\mathrm{T}}^{\mathrm{miss}} + \vec{p}_{\mathrm{T}}^{\ell_{\mathrm{W}}}\right|^2 + m_{\mathrm{W}}^2}\right]^2 - \left|\vec{p}_{\mathrm{T}}^{\ell\ell} + \vec{p}_{\mathrm{T}}^{\ell_{\mathrm{W}}}\right|^2$$

→ Events in the CR are categorized for the same N_j bins, and $\ell_W = e, \mu$.

Evidence for off-shell from $2\ell 2\nu + 4\ell$

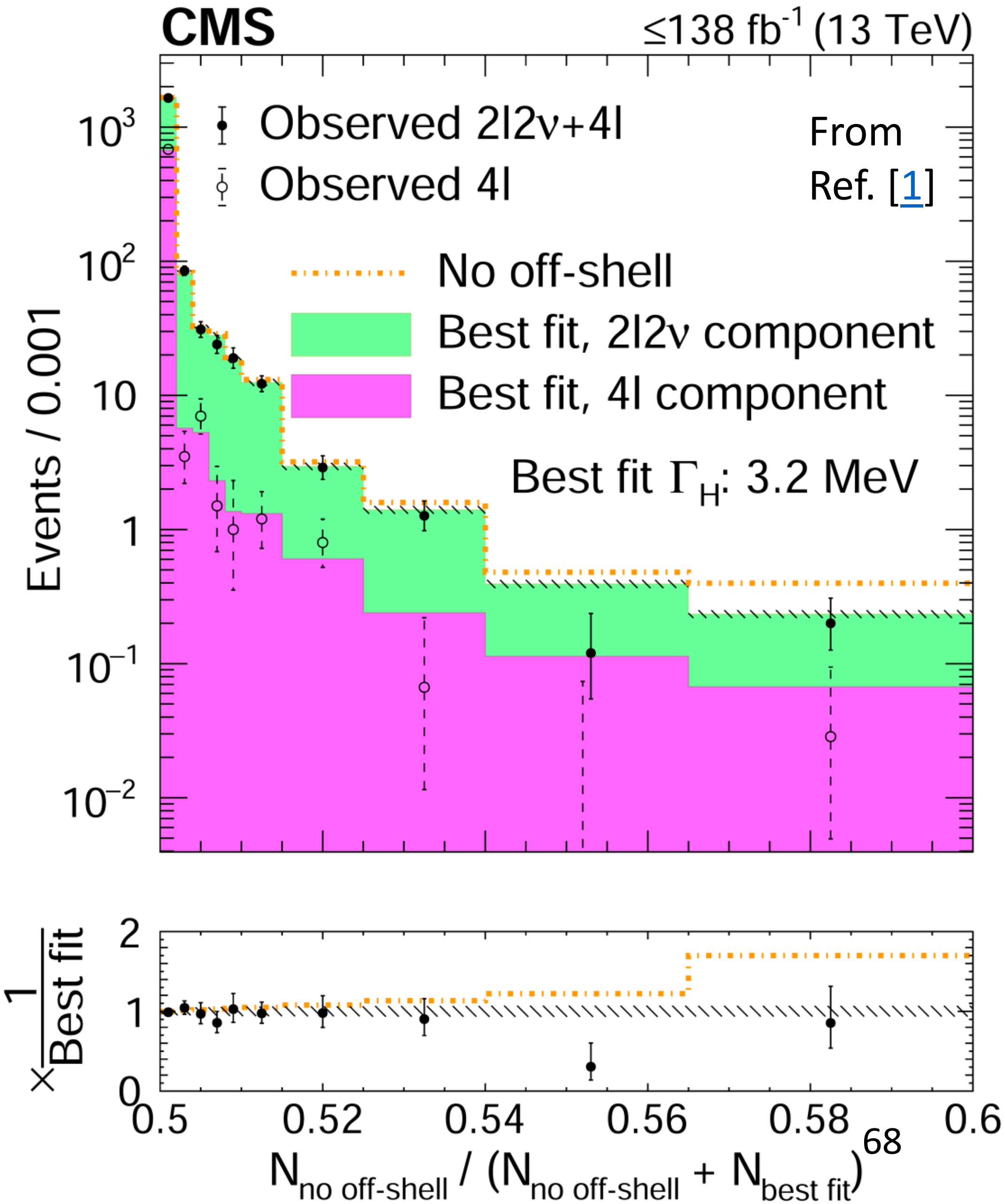

Plotted is a bin-by-bin ratio over the histograms of all observables and categories.

[1] CMS Collaboration; Nature Phys. 18 11 (2022)

Evidence for off-shell from $2\ell 2\nu + 4\ell$

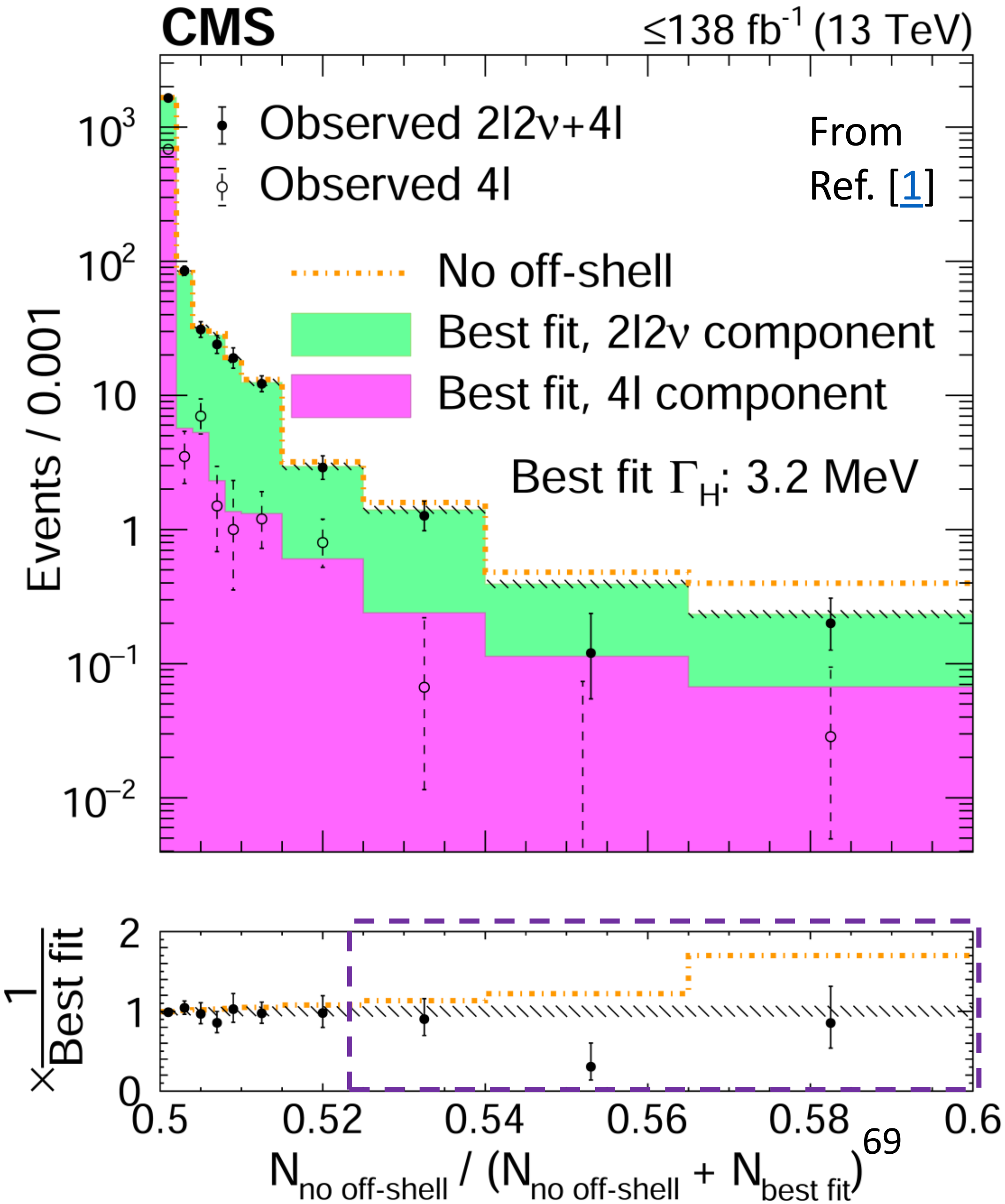

Plotted is a bin-by-bin ratio over the histograms of all observables and categories.

Once all bins and channels are considered, significance reaches 3.6 standard deviations.

[1] CMS Collaboration; Nature Phys. 18 11 (2022)

On-shell 4ℓ: ATLAS event selection

TRIGGER	
Combination of single-lepton, dilepton and trilepton triggers	
LEPTONS AND JETS	
ELECTRONS	$E_T > 7$ GeV and $\|\eta\| < 2.47$
MUONS	$p_T > 5$ GeV and $\|\eta\| < 2.7$, calorimeter-tagged: $p_T > 15$ GeV
JETS	$p_T > 30$ GeV and $\|\eta\| < 4.5$
QUADRUPLETS	
All combinations of two same-flavour and opposite-charge lepton pairs - Leading lepton pair: lepton pair with invariant mass m_{12} closest to the Z boson mass m_Z - Subleading lepton pair: lepton pair with invariant mass m_{34} second closest to the Z boson mass m_Z Classification according to the decay final state: 4μ, $2e2\mu$, $2\mu2e$, $4e$	
REQUIREMENTS ON EACH QUADRUPLET	
LEPTON RECONSTRUCTION	- Three highest-p_T leptons must have p_T greater than 20, 15 and 10 GeV - At most one calorimeter-tagged or stand-alone muon
LEPTON PAIRS	- Leading lepton pair: $50 < m_{12} < 106$ GeV - Subleading lepton pair: $m_{min} < m_{34} < 115$ GeV - Alternative same-flavour opposite-charge lepton pair: $m_{\ell\ell} > 5$ GeV - $\Delta R(\ell, \ell') > 0.10$ for all lepton pairs
LEPTON ISOLATION	- The amount of isolation E_T after summing the track-based and 40% of the calorimeter-based contribution must be smaller than 16% of the lepton p_T
IMPACT PARAMETER SIGNIFICANCE	- Electrons: $\|d_0\|/\sigma(d_0) < 5$ - Muons: $\|d_0\|/\sigma(d_0) < 3$
COMMON VERTEX	- χ^2-requirement on the fit of the four lepton tracks to their common vertex
SELECTION OF THE BEST QUADRUPLET	
- Select quadruplet with m_{12} closest to m_Z from one decay final state in decreasing order of priority: 4μ, $2e2\mu$, $2\mu2e$ and $4e$ - If at least one additional (fifth) lepton with $p_T > 12$ GeV meets the isolation, impact parameter and angular separation criteria, select the quadruplet with the highest matrix-element value	
HIGGS BOSON MASS WINDOW	
- Correction of the four-lepton invariant mass due to the FSR photons in Z boson decays - Four-lepton invariant mass window in the signal region: $115 < m_{4\ell} < 130$ GeV - Four-lepton invariant mass window in the sideband region: $105 < m_{4\ell} < 115$ GeV or $130 < m_{4\ell} < 160$ (350) GeV	

[1] ATLAS Collaboration; EPJC 80 957 (2020)
Errata: EPJC 81 29 (2021), EPJC 81 398 (2021)

ATLAS systematic uncertainties

Process	Uncertainty	Final State	Value (%)
	ggF Signal Region		
$qq \to ZZ$	QCD Scale	$2\ell 2\nu$	4–40
$qq \to ZZ + 2j$	QCD Scale	4ℓ	21–28
$qq \to ZZ + 2j$	QCD Scale	$2\ell 2\nu$	22–37
$qq \to ZZ + 2j$	Parton Shower	$2\ell 2\nu$	1–67
$gg \to H^* \to ZZ$	Parton Shower	4ℓ	27
$gg \to H^* \to ZZ$	Parton Shower	$2\ell 2\nu$	8–45
$gg \to ZZ$	Parton Shower	4ℓ	38
$gg \to ZZ$	Parton Shower	$2\ell 2\nu$	6–43
$WZ + 0j$	QCD Scale	$2\ell 2\nu$	1–54
	1-jet Signal Region		
$gg \to H^* \to ZZ$	Parton Shower	4ℓ	27
$gg \to H^* \to ZZ$	QCD Scale	$2\ell 2\nu$	13–18
$gg \to ZZ$	Parton Shower	4ℓ	38
$gg \to ZZ$	QCD Scale	$2\ell 2\nu$	18–20
$qq \to ZZ$ (EW)	QCD Scale	$2\ell 2\nu$	7–18
	2-jet Signal Region		
$qq \to ZZ + 2j$	QCD Scale	4ℓ	18–26
$qq \to ZZ + 2j$	QCD Scale	$2\ell 2\nu$	8–32
$gg \to H^* \to ZZ$	Parton Shower	4ℓ	27
$gg \to ZZ$	Parton Shower	4ℓ	38
$gg \to ZZ$	QCD Scale	$2\ell 2\nu$	18–20
$WZ + 2j$	QCD Scale	$2\ell 2\nu$	20–22
	$qq \to ZZ$ Control Regions		
$qq \to ZZ + 2j$	QCD Scale	4ℓ	26
	Three-lepton Control Regions		
$WZ + 2j$	QCD Scale	$2\ell 2\nu$	28

[1] ATLAS Collaboration; arxiv:2304.01532 (2023)

ATLAS systematic uncertainties

Systematic Uncertainty Fixed	$\mu_{\text{off-shell}}$ value at which $-2\ln\lambda(\mu_{\text{off-shell}}) = 4$
Parton shower uncertainty for $gg \to ZZ$ (normalisation)	2.26
Parton shower uncertainty for $gg \to ZZ$ (shape)	2.29
NLO EW uncertainty for $qq \to ZZ$	2.27
NLO QCD uncertainty for $gg \to ZZ$	2.29
Parton shower uncertainty for $qq \to ZZ$ (shape)	2.29
Jet energy scale and resolution uncertainty	2.26
None	2.30

Upper limits for $\mu^{\text{off-shell}}$ at 95% CL with most impactful systematics fixed:
→ Larger deviation indicates more impact

[1] ATLAS Collaboration; arxiv:2304.01532 (2023)

ATLAS systematic uncertainties

Process	Uncertainty	Final State	Value (%)
	ggF Signal Region		
$qq \to ZZ$	QCD Scale	$2\ell 2\nu$	4–40
$qq \to ZZ + 2j$	QCD Scale	4ℓ	21–28
$qq \to ZZ + 2j$	QCD Scale	$2\ell 2\nu$	22–37
$qq \to ZZ + 2j$	Parton Shower	$2\ell 2\nu$	1–67
$gg \to H^* \to ZZ$	Parton Shower	4ℓ	27
$gg \to H^* \to ZZ$	Parton Shower	$2\ell 2\nu$	8–45
$gg \to ZZ$	Parton Shower	4ℓ	38
$gg \to ZZ$	Parton Shower	$2\ell 2\nu$	6–43
$WZ + 0j$	QCD Scale	$2\ell 2\nu$	1–54
	1-jet Signal Region		
$gg \to H^* \to ZZ$	Parton Shower	4ℓ	27
$gg \to H^* \to ZZ$	QCD Scale	$2\ell 2\nu$	13–18
$gg \to ZZ$	Parton Shower	4ℓ	38
$gg \to ZZ$	QCD Scale	$2\ell 2\nu$	18–20
$qq \to ZZ$ (EW)	QCD Scale	$2\ell 2\nu$	7–18
	2-jet Signal Region		
$qq \to ZZ + 2j$	QCD Scale	4ℓ	18–26
$qq \to ZZ + 2j$	QCD Scale	$2\ell 2\nu$	8–32
$gg \to H^* \to ZZ$	Parton Shower	4ℓ	27
$gg \to ZZ$	Parton Shower	4ℓ	38
$gg \to ZZ$	QCD Scale	$2\ell 2\nu$	18–20
$WZ + 2j$	QCD Scale	$2\ell 2\nu$	20–22
	$qq \to ZZ$ Control Regions		
$qq \to ZZ + 2j$	QCD Scale	4ℓ	26
	Three-lepton Control Regions		
$WZ + 2j$	QCD Scale	$2\ell 2\nu$	28

Ranges of values of most dominant uncertainties in each N_j bin of ATLAS analyses

[1] ATLAS Collaboration; arxiv:2304.01532 (2023)